Earth Sciences New Zealand

Storm-River Flood Connectivity Analysis in Northland

Prepared for Northland Regional Council

April 2026

Prepared by:
Shailesh Singh, Rasool Porhemmat, George Griffiths

For any information regarding this report please contact:
Shailesh Singh
Hydrologist
Hydrology
+64 3 343 8053
Shailesh.Singh@niwa.co.nz

New Zealand Institute for Earth Science Limited
PO Box 8602
Riccarton
Christchurch 8440

Phone +64 3 348 8987

Client Report No: 2026091CH
Report date: April 2026
Project No: ELF26502

Revision	Description	Date
Version 1.0	Final version sent to client	29 April 2026
Version 1.1	Amendments completed and final version sent to client	12 June 2026

Quality Assurance Statement		
	Reviewed by:	Emily Lane
	Formatting checked by:	Rachel Wright
	Approved for release by:	Charles Pearson

© New Zealand Institute for Earth Science Limited ("Earth Sciences New Zealand") 2025. All rights reserved. This publication may not be reproduced or copied in any form without the permission of the copyright owner(s). Such permission is only to be given in accordance with the terms of the client's contract with Earth Sciences New Zealand. This copyright extends to all forms of copying and any storage of material in any kind of information retrieval system.

Whilst Earth Sciences New Zealand has used all reasonable endeavours to ensure that the information contained in this document is accurate, Earth Sciences New Zealand does not give any express or implied warranty as to the completeness of the information contained herein, or that it will be suitable for any purpose(s) other than those specifically contemplated during the project or agreed by Earth Sciences New Zealand and the client.

Contents

Executive summary **5**

1 Background and Rationale **7**

1.1 Why Northland needs a storm flood classification 7

1.2 Why a climate pattern analysis is operationally useful 8

1.3 Objectives 8

2 Data used in this study **10**

3 Method **13**

3.1 Flood and Storm event identification 13

3.2 Storm classification and event typology 14

3.3 Moisture transport and atmospheric drivers 15

3.4 Calculation of Integrated Vapour Transport (IVT) 17

3.5 Flood type classification 18

3.6 Climate mode classification (ENSO and SAM) 18

4 Results and discussion **20**

4.1 Seasonal distribution of widespread events 21

4.2 Temporal evolution of network coverage 21

4.3 Storm analysis 28

4.4 Integrated Analysis of Classified Flood Types and Event Characteristics 32

4.5 Influence of ENSO and SAM on flood behaviour 39

4.6 Operational implications for NRC 41

5 Recommendations for future work **44**

6 Conclusions **46**

7 Acknowledgements **48**

8 Glossary of abbreviations and terms **49**

9 References **50**

Appendix A Descriptive statistics of sites used in this study **52**

Appendix B Spatial coverage of daily events exceeding 10-year threshold **57**

Appendix C **Identified Events with ENSO and SAM index 63**

Appendix D **Site and frequency of events 68**

Tables

Table 2-1: Details of flow records used (1954-2025). 11
Table 4-1: Seasonal distribution of identified widespread hydrological events, 21
Table 4-2: Decadal summary of widespread hydrological events, 22
Table 4-3: Top 10 sites which have seen more frequent flood more than 10-year return period flood. 25
Table 4-4: The table summarises the number of monitoring sites classified into each flood hydrograph type. 32
Table 4-5: Distribution of flood spread by ENSO phase for identified flood events in Northland. 40
Table 4-6: Distribution of flood spread by SAM phase for identified flood events in Northland. 41
Table 4-7: Decision-support table linking storm type, flood type, and NRC operational response. 43

Figures

Figure 2-1: Location of flow gauges. 12
Figure 3-1: Study domain used for the atmospheric moisture transport analysis. The domain (20°S–60°S, 130°E–180°E) used in this study 17
Figure 4-1: Four large events and spatial distribution of events. 27
Figure 4-2: ERA5 integrated vapour transport (IVT) fields for the 18 August 2022 winter event at 3-hourly intervals (NZST), 30
Figure 4-3: ERA5 integrated vapour transport (IVT) fields for the 29 January 2011 summer event at 3-hourly intervals (NZDT). 31
Figure 4-4: Representative flood hydrographs for the three flood hydrograph types. 33
Figure 4-5: Conceptual schematic of flood hydrograph classification and catchment response behaviour. 33
Figure 4-6: Spatial distribution of flood hydrograph types across the study area. 36
Figure 4-7: Spatial distribution of normalised flood frequency. 37
Figure 4-8: Decision-support framework linking storm type to expected flood characteristics in Northland. 42

Executive summary

Northland experiences frequent flooding that poses risks to communities, infrastructure, ecosystems, and regional resilience. Flood impacts vary widely depending on storm characteristics, catchment response, and antecedent conditions. Generally, these dependencies are not always explicitly accounted for in flood planning and operational decision making. This report addresses this gap by developing an integrated framework to systematically link storm characteristics, climate drivers, and river flood responses across Northland.

The study presents a Northland Storm-Flood Typology that classifies flood-generating storms by their dominant meteorological triggers (including atmospheric rivers, extra-tropical cyclones, frontal systems, and localised convective storms) and links these storm types to three characteristic flood hydrograph types. Flood responses were analysed at 65 river gauging sites across Northland using long-term flow records and event-based metrics describing peak flow, response timing, and flood duration. Widespread flood events were most frequent during the 1960s–1980s. In recent decades, fewer events have occurred, but several have been more extreme and high impact.

Across Northland region, the two most common hydrograph flood types seen are rapid onset (Type 2) and slow response (Type 3), accounting for 75% of monitored sites. Specifically, Type 2 floods are characterised by rapid onset and pronounced peak flows with moderately extended recession periods, while Type 3 floods exhibit slower but sustained responses associated with prolonged rainfall. Type 1 floods, representing short-duration and lower-volume responses, are less common and tend to be confined to smaller or more efficiently drained catchments.

Spatial analysis indicates that flood hydrograph types are not evenly distributed across Northland. Type 2 flood behaviour is widespread, reflecting the prevalence of catchments that respond quickly to intense or spatially coherent rainfall. In contrast, Type 3 responses show spatial clustering in areas with greater catchment storage, flatter terrain, or enhanced floodplain connectivity, making them particularly susceptible to prolonged inundation.

Analysis of atmospheric drivers shows a strong link between persistent large scale moisture transport (diagnosed using integrated vapour transport) and the most spatially extensive flood events. Winter events dominated by prolonged synoptic forcing and atmospheric river-like conditions are substantially more spatially coherent than summer events, which are more often associated with short-duration, localised rainfall. These findings confirm that the persistence and coherence of moisture transport, rather than peak intensity alone, are key drivers of widespread flooding in Northland.

The study also examines the influence of large-scale climate patterns, particularly El Niño–Southern Oscillation (ENSO) and the Southern Annular Mode (SAM), on storm frequency and flood behaviour. Results indicate that climate phases may modulate the likelihood of different storm and flood types, providing an opportunity to support phase aware flood preparedness and planning.

Overall, this report delivers a transferable and operationally relevant framework for understanding flood behaviour in Northland. By explicitly linking storm type, climate drivers, catchment response, and flood hydrograph characteristics, the storm flood typology supports improved flood risk assessment, infrastructure design, early warning, and climate-informed regional planning. The findings provide NRC with a sound evidence base to better anticipate flood impacts and tailor management strategies to dominant flood mechanisms across the region.

1 Background and Rationale

1.1 Why Northland needs a storm flood classification

Northland experiences a highly variable climate characterised by warm, humid summers, mild winters, and frequent wind exposure. Rainfall occurs throughout the year, punctuated by episodic heavy rainfall events that can generate significant flooding (Chappell, 2013). Mean annual rainfall varies markedly across the region, with hilly areas north of Dargaville and Kaikohe receiving approximately 2000 mm yr^{-1}, compared with around 900 mm yr^{-1} near Cape Reinga. Interannual variability is also substantial; for example, annual rainfall totals at Dargaville ranged from 800 mm to 1600 mm during the period 1951–1985, while there was considerable annual variability but no long-term trend is evident at Waimatenui south of Kaikohe over the period 1914–2000 (Chappell, 2013).

Northland commonly experiences summer dry spells lasting two to three weeks, driven by persistent anticyclones over or east of Australia. These systems are often followed by weak frontal activity along their southern margins, producing cloudy conditions with little or no rainfall. The repetition of this circulation pattern can generate extended dry periods, typically between December and March. More severe droughts are generally associated with slow moving or blocking high pressure systems over the Tasman Sea and Northland, although the persistence of these systems and their hydrological impacts are not fully understood (Singh *et al*. 2021).

Despite these dry periods, Northland is also highly prone to flooding due to its peninsular geography, proximity to warm oceanic moisture sources, short and steep headwater catchments, and estuary-controlled river outlets. These characteristics promote rapid river rises during intense rainfall and slow recession of floodwaters where drainage is impeded at tidal outlets (Chappell 2013, McKerchar and Henderson 2003, Woods and McKerchar 2003). Historical storm-types that have caused damaging floods include extra-tropical cyclones, North Tasman lows, and localised convective storms, with rainfall often substantially enhanced by orographic lifting on windward slopes (Revell et al. 2016, Sinclair 2002, Gray 2003). Large, region-spanning storm events can simultaneously stress transport, power, communication, and water supply networks, complicating emergency response and recovery (Bollinger and Kennedy 2012).

The contrasting nature of Northland's flood hazards was clearly demonstrated in February 2023. Cyclone Gabrielle (12–13 February 2023) produced prolonged, late-loaded rainfall that resulted in record 24–48 h flows at many river gauges. In contrast, the Mangawhai flash flood (25 February 2023) was driven by a short-duration, highly localised convective rainfall burst with intensities approaching 100 mm h^{-1} and lag times of just 2–4 hours. Together, t
hese events highlight that different meteorological archetypes can produce fundamentally different flood responses, which in turn require distinct operational triggers, design assumptions, and risk-management strategies (Merz et al. 2014, Zscheischler et al. 2020).

Developing a systematic storm flood classification provides a consistent framework for capturing this diversity in flood behaviour. By linking storm characteristics to catchment-scale

flood responses, such a classification enables clearer interpretation of past events and supports more robust, process-based flood management.

1.2 Why a climate pattern analysis is operationally useful

Large-scale climate models, particularly the El Niño–Southern Oscillation (ENSO) and the Southern Annular Mode (SAM), exert a strong influence on storm tracks, moisture transport pathways, and storm persistence affecting northern New Zealand. In Northland, precipitation variability shows clear co-variation with ENSO indices, with La Niña conditions generally favouring wetter outcomes and more frequent easterly flow regimes. These circulation patterns enhance the likelihood of atmospheric river landfalls and orographic rainfall enhancement, particularly along the eastern parts of the region (Prince et al. 2021).

SAM phases further influence the latitudinal positioning and persistence of synoptic systems, potentially modifying both the frequency and spatial focus of heavy rainfall and flooding. Understanding how these climate patterns modulate storm type, rainfall duration, and moisture supply is therefore directly relevant to flood preparedness. Quantifying these relationships enables climate-aware readiness, such as adjusting operational thresholds, situational awareness, and resource allocation in anticipation of increased flood risk during forecast La Niña or favourable SAM phases (Comola et al. 2021).

1.3 Objectives

This study is designed to address the need for an integrated understanding of storm drivers, flood response, and climate controls in Northland. The specific objectives are to:

1. Storm flood classification
   Develop a systematic and objective classification of historical storms based on their dominant meteorological triggers and intensity and quantify how each storm class translates into characteristic flood responses across Northland's river catchments, with a focus on sites supported by robust long-term flow records.

2. Climate pattern analysis
   Quantify the influence of ENSO and SAM on storm frequency, storm-type composition, atmospheric river occurrence, rainfall intensity and duration, and flood severity, including the assessment of conditional extremes and the mediating role of persistent moisture transport.

Building on the climatic context and flood management challenges outlined above, this study adopts an integrated ,and event based methodological framework to explicitly link storm drivers, climate variability, and observed river flood responses across Northland. A comprehensive suite of hydrological, meteorological, and atmospheric datasets was assembled to support consistent identification of flood events, characterisation of storm properties, and assessment of large-scale climate influences. These datasets provide sufficient temporal coverage, spatial extent, and resolution to capture both short-duration localised floods and long-duration, regionally coherent events, while accounting for changes in

monitoring network availability through time. The methodological approach prioritises objective, reproducible classification schemes and metrics that are transferable to operational and planning contexts, enabling robust storm flood classification and climate pattern analysis as described in the following sections.

2 Data used in this study

River flow data were obtained from Earth Sciences New Zealand (ESNZ) and the Northland Regional Council (NRC) and form the primary basis for the flood analyses presented in this report. Details of all available flow monitoring sites and their attributes are provided in Table 2-1, with data availability and descriptive statistics summarised in Appendix A.

A total of 71 flow monitoring sites were initially considered for inclusion. Sites with less than five years of valid flow records were excluded to avoid statistical instability in event identification and flood characterisation. Following this screening, 65 flow sites were retained for analysis. Record lengths across these sites range from 5 to 68 years, with a mean record length of 31 years, providing robust temporal coverage for event-based and climatological assessment. The spatial distribution of the retained flow gauges is shown in Figure 2-1. While a minimum threshold of five years of record length was adopted to retain a sufficient number of sites for analysis, it is acknowledged that shorter records introduce greater uncertainty in the estimation of flood frequency parameters. In particular, fitting a Generalised Extreme Value (GEV) distribution to short time series can result in highly variable parameter estimates, especially for the shape parameter, which strongly influences the estimation of extreme return levels. Consequently, return period estimates derived from sites with limited data should be interpreted with caution.

Flow observations were processed at a daily time scale, consistent with the objectives of identifying flood events, characterising hydrograph response, and linking river responses to storm-scale and large-scale climate drivers.

Rainfall and temperature data were sourced from ESNZ, NRC, and the New Zealand Meteorological Service (NZMS). Rainfall data were also aggregated to a daily time scale to ensure consistency with the flow records and to support storm and hydrograph classification. From the 301 rainfall monitoring sites available across Northland, the nearest rainfall gauge to each flow site (rain site can be within the catchment or outside) was arbitrarily selected to represent catchment-scale precipitation conditions. This approach provides a practical and spatially consistent representation of rainfall forcing at each river site and is well suited to the event-based analyses undertaken. It is acknowledged that representing catchment rainfall using a single nearest gauge introduces uncertainty, as it may not fully capture spatial variability in rainfall, particularly for localised or convective events and in areas with complex topography, or where rainfall near a catchment outlet is not typical of rainfall within the catchment. This limitation is inherent in gauge-based approaches and may influence the representation of rainfall inputs at some sites. However, the method was considered appropriate for the regional, event-based analysis undertaken in this study.

Rainfall data were used primarily to support flood hydrograph typology, including the interpretation of event duration, intensity, and timing relative to observed river responses. Temperature data were used to provide additional hydrometeorological context where relevant, although rainfall and flow variables form the core of the flood classification and analysis framework.

In general hydrological applications, temperature is an important variable used to distinguish precipitation phase (rainfall versus snow), which can influence runoff generation and hydrograph response. In this study, temperature data were retained for this purpose within the framework. However, this distinction is not relevant for the Northland region, where snowfall does not occur. Therefore, temperature does not directly influence the results presented here and is used primarily for completeness and consistency of the methodology.

In addition to hydrometeorological data, catchment characteristics were derived to support interpretation of flood responses and spatial variability. These characteristics were extracted from a digital elevation model (DEM), land-use datasets, soil maps, and the River Environment Classification (REC) review classification. Together, these datasets provide information on catchment topography, land cover, soil properties, and hydrological setting, enabling flood hydrograph behaviour to be interpreted in the context of underlying physical and land-use controls.

Table 2-1: Details of flow records used (1954-2025).

Number of Sites	Record Length (years)			Mean Annual Flow (m^3/s)		
	Maximum	Minimum	Mean	Maximum	Minimum	Mean
65	68	6	31	422	0.530	51.7

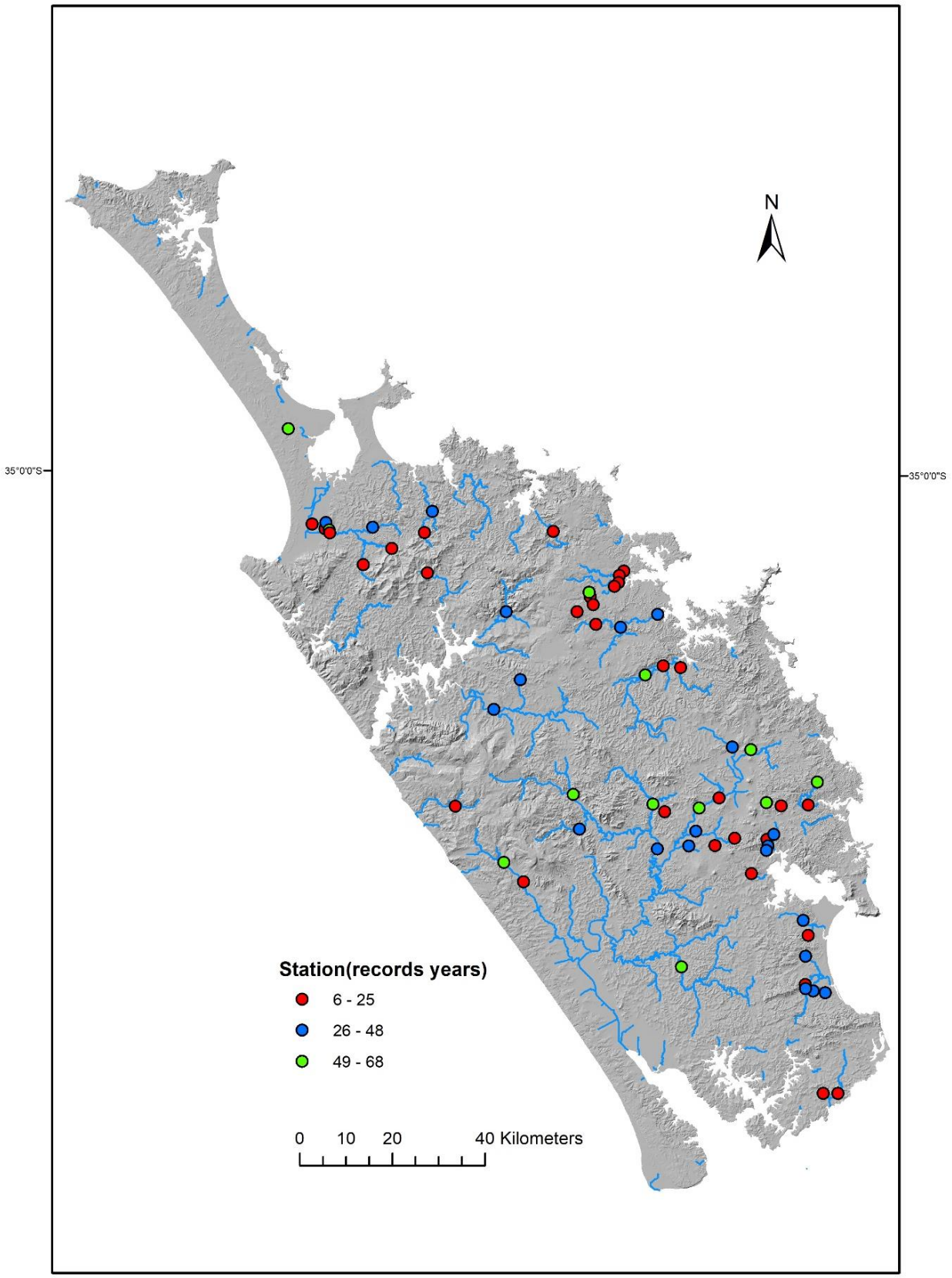


Figure 2-1: Location of flow gauges.

3 Method

3.1 Flood and Storm event identification

Rainfall and river flow data were obtained for all available monitoring sites. An initial data screening was undertaken to assess record length and data completeness. No gap-filling was applied to either rainfall or flow datasets, and analyses were conducted using observed data only. This approach was adopted to avoid introducing artificial values that may bias flood magnitude and timing, particularly for extreme events. As a result, data completeness varies between sites, and records with missing observations were retained where sufficient data were available for analysis. Sites with less than five years of flow data were excluded from further analysis to avoid statistical instability and bias in the flood frequency analysis.

The following steps were then undertaken in this study:

1. Descriptive statistics were calculated for each flow site, including the mean, median, maximum, standard deviation, and the number of years of available data.
2. A Generalised Extreme Value (GEV) distribution was fitted to the annual maximum flow series at each site to estimate the 10-year return period flow.
3. For each site, all flow events exceeding the estimated 10-year return period threshold were identified. The dates of these exceedance events were recorded, and an event database was compiled across all sites.
4. The event database was then filtered to identify unique events, noting that several exceedances occurred on common dates across multiple sites, indicating spatially coherent flood events.
5. Based on the identified unique event dates, all flood events with return periods greater than 10 years were collated, and corresponding storm rainfall maps were obtained for each event date.
6. Finally, the identified flood events and their corresponding storm rainfall patterns were analysed jointly to examine the relationship between extreme flows and storm characteristics.

All flood events exceeding the site-specific 10-year return period threshold were identified, and the dates of exceedance were recorded. These exceedances were compiled into a multi-site event database. Because exceedances frequently occurred on the same calendar dates across multiple sites, the database was filtered to identify unique regional flood events, representing spatially coherent hydrological responses rather than isolated site-specific behaviour.

For each identified regional event, all flood occurrences with return periods greater than 10 years were collated, and corresponding storm rainfall data were extracted for the event period. These flood events and their associated rainfall patterns form the basis for examining the relationship between storm characteristics and river flood responses.

The 10-year return period threshold was selected as a practical benchmark to identify significant flood events while retaining a sufficient number of events for regional analysis. It is

acknowledged that the selection of this threshold may influence the number and characteristics of identified events, and alternative thresholds (e.g. 20-year or 50-year return periods) could yield different event sets and interpretations of spatial coherence and seasonality.

While the methodological framework applied in this study is readily transferable to other return period thresholds, a formal sensitivity analysis of threshold selection is beyond the scope of the present work. The results should therefore be interpreted in the context of the chosen 10-year return period threshold.

3.2 Storm classification and event typology

Historic storms impacting Northland were systematically classified according to their dominant meteorological trigger, resulting in a structured Northland Storm-Flood-Typology. This typology is designed to explain why, where, and how different storm types generate distinct flood characteristics, such as rapid flashy responses versus basin-filling floods, tide-impeded versus free-draining behaviour, and debris-rich versus clear-water flows. The classification is intended to be operationally interpretable and supported by spatial mapping and objective decision rules.

Each flood event was assigned one primary storm trigger class and, where appropriate, one or more secondary tags. Trigger assignment was based on objective criteria traceable to the available datasets, supported by synoptic interpretation and atmospheric diagnostics.

The storm trigger classes adopted in this study are defined as follows:

Class 1 – Atmospheric River (AR)
A land-falling atmospheric river was identified when Integrated Vapour Transport (IVT) (see Section 3.4 for definition) exceeded a threshold of approximately 250–400 kg m^{-1} s^{-1} for at least 12 hours over a moisture corridor typically ≥1500 km long and ≥400 km wide intersecting Northland. AR occurrence was based on the atmospheric river catalogue adopted in this study (UCLA dataset), verified using ERA5 IVT composites. If AR conditions were present for ≥50% of the event duration, the AR flag was set to TRUE.

Class 2 – Tropical / Extra-tropical Cyclone (TC/ETC)
Events were classified as TC/ETC when event dates overlapped an IBTrACS (International Best Track Archive for Climate Stewardship) cyclone track (Knapp et al. 2010, Pfahl and Wernli 2012) passing within 500 km of Northland or where national agency records identified tropical or extra-tropical cyclone impacts. Classification was supported by synoptic indicators such as tight mean sea-level pressure gradients and warm conveyor belt signatures. Northland experiences relatively high exposure, with approximately one ETC per year passing within this distance.

Class 3 – North Tasman Low / Frontal Rainband
This class includes deepening lows over the northern Tasman Sea associated with strong frontal

rainbands and slow system propagation across Northland. Events undergoing rapid cyclogenesis ("weather bombs"), defined by central pressure falls exceeding 24 hPa in 24 hours, were also included within this class. Orographic enhancement associated with persistent northeasterly or easterly flow was identified separately using secondary process tags.

Class 4 – Localised Convective Outbreak / Squall Line
Localised convective events were identified using sub-regional radar signatures of back-building cells or linear convective systems producing short-duration rainfall extremes. For classification purposes, events were required to produce ≥40 mm of rainfall in 1 hour at one or more gauges. Rainfall intensities associated with this class typically ranged from 40 to 60 mm in 1 hour, with higher local totals observed in exceptional cases. These events often coincided with sea-breeze convergence or mesoscale lifting. An observed rainfall total of 109.4 mm in 1 hour at Leigh was used as a canonical reference case to illustrate the upper bound of this class

Secondary event tags were applied where relevant, including orographic enhancement, compound coastal–fluvial effects, pre-saturated soils, debris-rich flows, and thunder or lightning observations.

Based on storm trigger classes described above, storm events were classified according to their dominant meteorological driver using a structured storm–flood typology. Each event was assigned one primary storm type: *(i)* extra-tropical cyclone with atmospheric river influence (ETC + AR), *(ii)* extra-tropical cyclone without sustained atmospheric river influence (ETC), or *(iii)* localised convective storm. In the event classification used in the results, North Tasman Low and frontal rainband systems are included within the broader extra-tropical cyclone (ETC) category due to their similar synoptic characteristics. Classification was based on a combination of atmospheric diagnostics, rainfall characteristics, and synoptic context. Only a subset of events were individually classified using detailed atmospheric and rainfall diagnostics; the remaining events were assigned a default convective classification where data were insufficient, and this should be interpreted as a limitation of the dataset.

3.3 Moisture transport and atmospheric drivers

To characterise the large-scale atmospheric conditions associated with spatially coherent flood events, the analysis focused on Integrated Vapour Transport (IVT) as a diagnostic of moisture transport pathways and storm persistence. Integrated Vapour Transport measures the total horizontal transport of water vapour through the atmospheric column and is commonly used to identify atmospheric rivers.

Atmospheric variables were obtained from the ERA5 reanalysis dataset (Hersbach et al. 2018 and 2020) produced by the European Centre for Medium-Range Weather Forecasts (ECMWF). ERA5 provides hourly atmospheric fields at a spatial resolution of approximately 0.25 ° (~31 km) and integrates numerical weather prediction output with observational data to reconstruct historical atmospheric conditions.

The variables used in this analysis include:

- Zonal wind component (*u*).
- Meridional wind component (*v*).
- Specific humidity (*q*).

These variables were extracted at multiple pressure levels and used to compute vertically integrated moisture transport.

Atmospheric variables were extracted from the ERA5 reanalysis dataset over a domain spanning from 60 S to 20 S and130 E to 180 E (Figure 3-1).

This domain captures the primary oceanic moisture source regions for New Zealand, including the subtropical South Pacific and the Tasman Sea, where strong moisture transport pathways often develop during extreme rainfall events. By analysing Integrated Vapour Transport (IVT) across this larger domain, it is possible to track the development and propagation of moisture plumes toward the Northland region.

The selected spatial extent ensures that both local atmospheric conditions and remote moisture sources contributing to extreme rainfall events are represented in the analysis. The longitudinal extent of the domain is intentionally biased toward regions west of New Zealand to capture upstream moisture source areas associated with the prevailing mid-latitude westerly circulation. In the New Zealand region, large-scale atmospheric flow is predominantly westerly, particularly during extreme rainfall events and atmospheric river conditions, resulting in moisture transport pathways that originate over the Tasman Sea and the broader subtropical western Pacific and propagate eastward toward the country (e.g., Hoskins and Ambrizzi, 1993; Shu et al., 2021). Consequently, extending the domain further east of New Zealand provides limited additional information on moisture source regions, as this area is typically downstream of the primary moisture transport pathways influencing the country. The selected domain therefore prioritises upstream regions where moisture uptake and transport are most relevant.

to extreme precipitation in New Zealand.

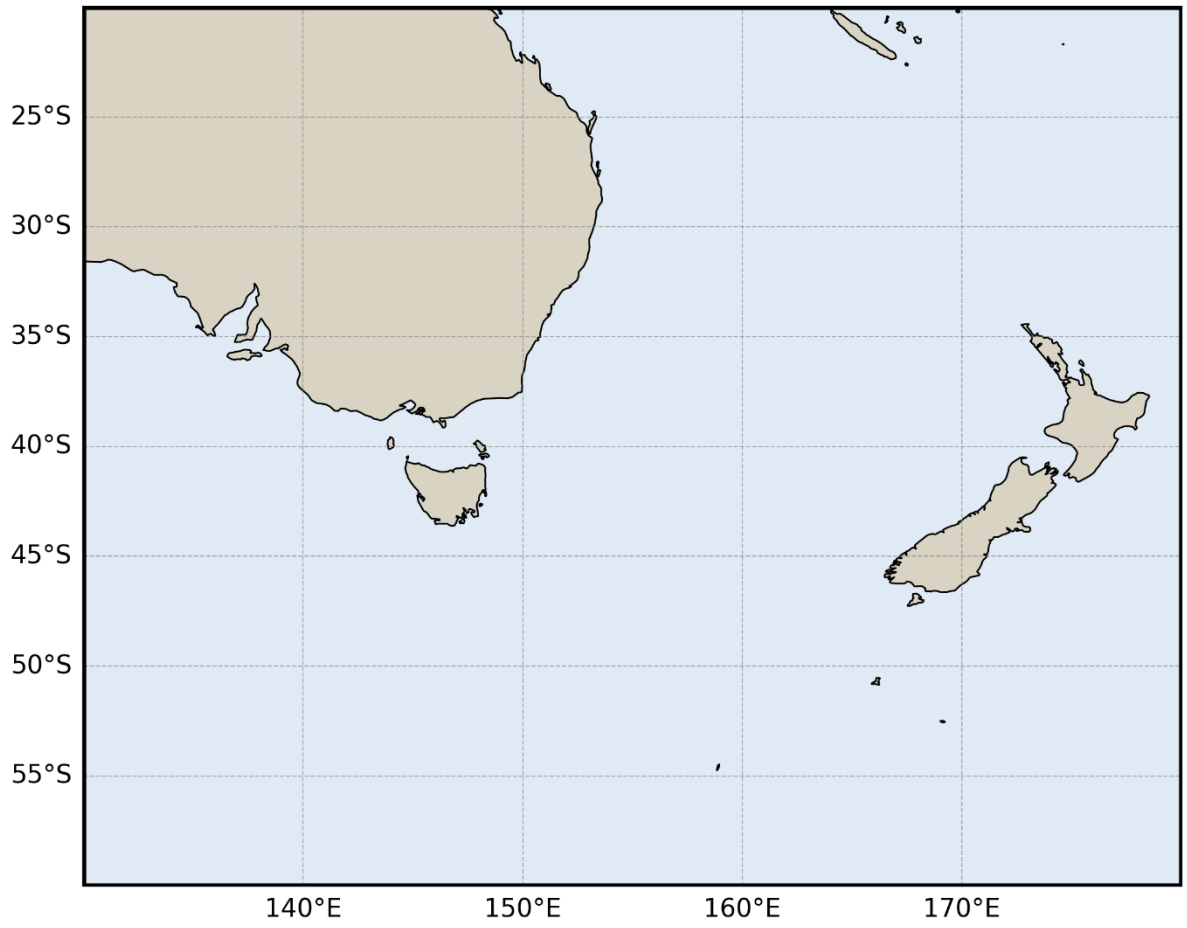


Figure 3-1: Study domain used for the atmospheric moisture transport analysis. The domain (20°S–60°S, 130°E–180°E) used in this study encompasses the Tasman Sea, the southwest Pacific Ocean, and New Zealand, allowing identification of large-scale moisture pathways associated with extreme rainfall events in Northland.

3.4 Calculation of Integrated Vapour Transport (IVT)

Integrated Vapour Transport (IVT) represents the vertically integrated horizontal transport of water vapour through the atmosphere. The IVT field was calculated over the domain from ERA5 pressure-level data following standard formulations used in atmospheric river studies. The resulting IVT fields describe both the magnitude and direction of horizontal moisture transport, allowing identification of persistent moisture corridors originating from the Tasman Sea and the subtropical South Pacific and impinging on northern New Zealand.

The magnitude of IVT is defined as:

$$IVT = \sqrt{\left(\frac{1}{g}\int_{1000\ hPa}^{300\ hPa} qu\ dp\right)^2 + \left(\frac{1}{g}\int_{1000\ hPa}^{300\ hPa} qv\ dp\right)^2} \qquad \text{Equation 1}$$

where g represents gravitational acceleration ($m\ s^{-2}$), q is the specific humidity ($Kg\ Kg^{-1}$), u and v are the zonal and meridional components of the wind ($m\ s^{-1}$), and p is pressure.

3.5 Flood type classification

Flood responses were classified based on hydrograph shape and timescale, recognising that different rainfall and catchment conditions generate characteristically different flood behaviours. Catchment and climate attributes such as topography, soil properties, land cover, and antecedent wetness play a critical role in controlling runoff generation, flood magnitude, and duration.

Hydrographs dominated by high-intensity rainfall typically exhibit short-duration, steep-rising limbs, and high peak flows, whereas long-duration rainfall sequences tend to produce prolonged flooding with larger volumes and slower recession. Small, steep catchments are therefore more prone to short-duration floods, while flatter or wetter catchments often experience sustained flood responses.

Flood events were classified using the R1/R2/R3 flood-type scheme of *Fischer et al.* (2025), which is based primarily on hydrograph time scale:

- R1 – Heavy rainfall floods: short duration, small volume, steep rising limb, large peaks.
- R2 – Moderate intensity/duration floods.
- R3 – Long-duration rainfall sequences: large volumes, often multi-peaked hydrographs.

Flood types defined in this study (Type 1, Type 2, Type 3) were mapped directly to the R1/R2/R3 scheme based on event-scale hydrograph statistics. Median event durations of approximately 5, 10, and 18 days for Types 1, 2, and 3, respectively, reproduce the short–medium–long response continuum at the monitored catchments. This classification enables flood behaviour to be interpreted consistently across the region and provides a structured basis for linking flood responses to storm type, catchment characteristics, and climate drivers.

3.6 Climate mode classification (ENSO and SAM)

To quantify the influence of large-scale climate variability on flood-producing storm events, each identified event was classified according to the contemporaneous phase of the El Niño–Southern Oscillation (ENSO) and the Southern Annular Mode (SAM). Monthly ENSO conditions were represented using the Niño 3.4 sea-surface temperature anomaly index obtained from the NOAA Climate Prediction Center, based on the ERSSTv5 dataset. Monthly SAM index values were obtained from the NOAA Physical Sciences Laboratory, calculated from zonal-mean sea-level pressure differences between 40° S and 65° S. Climate indices were matched to flood events according to the calendar month in which each event occurred.

ENSO phase classification was based on the monthly ENSO index value, with events classified as *El Niño* when the index exceeded +0.5, *La Niña* when the index was below −0.5, and *Neutral* otherwise. SAM phase classification followed an analogous approach, with events classified as *Positive* (index ≥ +0.7), *Negative* (index ≤ −0.7), or *Neutral*. These thresholds are consistent with standard practice in climate–hydrology studies and allow objective comparison of flood characteristics across climate phases (Marshall, 2003).

Climate phase classification enables event-scale analysis of how storm frequency, spatial coherence, and flood response types vary under different large-scale atmospheric regimes.

4 Results and discussion

Descriptive statistics were derived for each flow monitoring site to characterise the overall distribution of observed flows and the length of record available at each location. These statistics, including measures of central tendency, variability, and record length, are summarised for all sites in Appendix A and provide the contextual basis for subsequent event-based analyses.

Across the monitoring network, flow events exceeding the estimated 10-year return period threshold were identified at individual sites. When these exceedances were examined collectively, it was evident that many occurred on common dates across multiple sites, indicating the presence of spatially coherent flood events rather than isolated, site-specific responses. The consolidation of site-level exceedances into a single event database enabled the identification of unique regional events and facilitated assessment of their spatial extent.

A subset of these events, defined as those exceeding the 10-year return period threshold, is documented in Appendix B. This appendix provides details of the timing and site participation associated with each selected event and forms the basis for the network-scale analyses presented below. Using this curated event set, subsequent analyses focus on the seasonal distribution of widespread events, temporal changes in event representation, and the influence of monitoring network availability on the observed spatial coherence of extreme flows.

The results presented in the following sections are therefore interpreted in the context of both hydrological variability and the evolving structure of the monitoring network, allowing widespread flood behaviour to be assessed while accounting for known limitations in historical data coverage.

Widespread hydrological events were identified using a dataset of common event dates, where each event represents a calendar day on which concurrent responses were observed at multiple monitoring sites. For each event date, the number of responding sites (n_sites) was recorded alongside the list of contributing sites. To account for temporal changes in the monitoring network, site availability was explicitly quantified using station-level operational metadata, including start and end dates of valid observations.

Normalised coverage was calculated/estimated by the number of sites where the event occurred divided by the total number of sites operational at the time. This normalised coverage metric was used to enable comparison of event extent across periods with differing network density and data availability.

Seasonal classification was applied based on the calendar month of each event, using standard Southern Hemisphere seasons (summer: December–February; autumn: March–May; winter: June–August; spring: September–November). Events were summarised by season to assess intra-annual variability in the occurrence of widespread events. Temporal changes in network performance and event representation were examined by aggregating events by decade and summarising both the number of events and the distribution of coverage metrics within each decade.

All analyses were conducted using the R statistical computing environment. Summary statistics were calculated using both mean and median values to reduce sensitivity to skewed

distributions and to provide a robust representation of typical network coverage during widespread events.

4.1 Seasonal distribution of widespread events

The seasonal analysis indicates a clear dominance of widespread events during the winter period. Approximately 40% of all identified events occurred in winter, compared with 26% in summer, 24% in autumn, and only 10% in spring (Table 4.1).

This winter dominance reflects the prevalence of large-scale frontal systems and persistently wet synoptic conditions, which are more likely to generate spatially coherent flooding across multiple catchments. In contrast, spring exhibits the lowest frequency of widespread events, suggesting that transitional atmospheric conditions and lower catchment wetness limit the spatial extent of simultaneous responses.

Summer events, while less frequent than winter, still represent a substantial proportion of widespread events. These are likely associated with high-intensity rainfall systems, such as ex-tropical cyclones or atmospheric river events, which can produce extensive rainfall over short periods. Autumn shows a comparable contribution, potentially reflecting the increasing catchment wetness leading into winter.

Please note that the above interpretation is based primarily on qualitative reasoning supported by IVT case studies and general climatological understanding, and is not explicitly derived from the storm classification framework developed in this study.

Overall, the seasonal distribution highlights that widespread hydrological events are strongly controlled by large-scale climatic forcing and antecedent wetness, rather than purely localised rainfall processes.

Table 4-1: Seasonal distribution of identified widespread hydrological events, showing the number of events and the proportion of total events occurring in each Southern Hemisphere season.

Season	Number of Events	Percentage of total events (%)
Winter	48	40
Summer	32	26
Autumn	29	24
Spring	12	10

4.2 Temporal evolution of network coverage

The decadal analysis reveals substantial variation in both the number of detected events and the proportion of the monitoring network available at the time of each event.

During the 1960s–1980s, mean network coverage during events was particularly low, declining from approximately 11% in the 1960s to less than 5% in the 1980s. Median coverage values in these decades were even lower, indicating that most events were captured by only a very small fraction of the total potential network. This reflects the limited spatial density and shorter operational periods of monitoring sites during earlier decades.

From the 1990s onwards, a gradual improvement in coverage is evident. Mean coverage increased to approximately 7–9% in the 2000s–2020s, with higher median values, indicating a more consistently available network during recent events. Despite this improvement, coverage remains relatively modest, suggesting that even in recent decades, widespread events are often observed by only a subset of the full monitoring network.

Importantly, the number of detected events per decade does not increase monotonically with coverage, indicating that observed temporal patterns reflect both genuine hydro-climatic variability and the evolving structure of the monitoring network.

Temporal variability in network availability strongly affects interpretation of historical widespread flood events. Early-period events (particularly pre-1990) are likely to be systematically underestimated in spatial extent, as many sites were not operational at the time. Consequently, apparent increases in event coverage in recent decades should not be interpreted solely as changes in event magnitude or frequency, but also as a function of improved observational capacity.

Median coverage values are consistently lower than mean values across all decades, indicating that a small number of events with relatively high site availability can disproportionately influence average statistics. This reinforces the need to interpret long-term trends with caution and to consider normalised metrics, such as percentage network coverage, rather than raw site counts alone.

Table 4-2: Decadal summary of widespread hydrological events, including the number of events per decade and the mean and median proportion of the monitoring network available during each event

Decade	Number of Events	Mean Coverage percentage (%)	Median Coverage percentage (%)
1950*	1	33	33
1960	22	11	9
1970	21	7	6
1980	21	5	3
1990	11	5	3
2000	18	7	4
2010	10	9	7
2020++	17	9	4

* please note there were much fewer sites during this decade

++ please note this covers the first half of the 2020s

Table 4-2 summarises the decadal distribution of widespread hydrological events across Northland, together with the mean and median proportion of the monitoring network available during each event. The results indicate substantial temporal variability in both the frequency of widespread events and the extent of monitoring coverage.

The highest numbers of widespread events occur during the 1960s, 1970s and 1980s, each decade recording around 21–22 events. In contrast, the 1950s are represented by a single widespread event, reflecting both genuinely lower event detection and historically limited

monitoring infrastructure. Please also note that 1950s decade represents the second half of the 1950s as data monitoring stated in 1954.

Despite the relatively high number of events in earlier decades, network coverage was generally low. Median coverage declined steadily from 9% in the 1960s to 3% in the 1980s and 1990s, indicating that widespread flood behaviour during these periods is inferred from a limited number of gauges. This has implications for historical consistency, particularly when comparing the spatial coherence of floods across decades.

From the 2000s onward, a clear improvement in effective monitoring coverage is observed. Mean coverage increases to 7–9% in the 2000s, 2010s and 2020s, and median coverage improves from a low of 3–4% in earlier decades to 7% in the 2010s. Although the total number of widespread events in the 2010s is lower (10 events), this decade benefits from substantially improved spatial representation, increasing confidence in flood classification and network-scale interpretation.

Overall, Table 4-2 highlights two key points:

1. Widespread flooding is a persistent feature of Northland's hydrological record, occurring in every decade for which we have record.

2. Interpretation of historical events must explicitly account for monitoring limitations, particularly prior to the 1990s, as apparent changes in flood behaviour may partly reflect changes in network density rather than climatic forcing alone.

Table 4-3 identifies the top ten monitoring sites that have been affected most frequently by floods exceeding the ten-year return period. These sites represent locations that consistently respond during regionally significant flood events and therefore provide important insight into spatial flood coherence and network sensitivity. Additional sites with comparable event frequencies, including those tied at the lower ranks, are reported in Appendix D

The most frequently impacted sites Waiharakeke at Willowbank (3819), Whakapara at Cableway (46632), and Manganui at Permanent Station (46651) each appear in ten separate >10-year flood events, spanning multiple decades from the late 1960s to the early 2020s. This persistent recurrence indicates that these gauges are located in hydrologically responsive and regionally connected catchments, often responding to both cyclone-driven and prolonged large-scale rainfall events.

Several other sites, including Wairua at Purua (46644), Awanui at School Cut (1316), Waipapa at Forest Ranger (47804) and Opouteke at Suspension Bridge (1046651), record 8–9 major flood events. These sites are repeatedly activated during widespread storms such as the March 2007, January 2011, July 2020, and February 2023 events, reinforcing their importance as indicators of severe regional flooding.

The distribution of site Types across Table 4-3 shows that Types 2 and 3 sites dominate the ranking, reflecting a tendency for larger, lower-gradient or more integrated catchments to respond during long-duration and high-severity storms. In contrast, Type 1 sites appear less frequently, consistent with their typically localised or flashy response characteristics and lower likelihood of simultaneous activation across the wider region.

The temporal spread of event dates associated with these top ten sites demonstrates that:

- Major flood activity is not confined to a single climatic period but instead recurs across multiple decades.
- Recent decades (particularly the 2010s and 2020s) contribute disproportionately to the event lists of many sites, reflecting both improved monitoring coverage and an increase in high-impact storms affecting Northland.

Taken together, Tables 4-2 and 4-3 provide strong evidence that a relatively small subset of gauges consistently captures the majority of regionally significant flood events. These sites function effectively as sentinel gauges for widespread flooding and are highly valuable for:

- validating flood typologies,
- understanding spatial coherence of extreme events,
- and supporting operational flood response and post-event review.

However, the results also emphasise the need for caution when interpreting long-term trends. Apparent increases in flood frequency in recent decades may partly reflect improved network density and data availability, rather than purely climatic changes. Consequently, future analyses should continue to combine storm-scale classification, climate context, and network coverage metrics to ensure robust interpretation of flood risk in Northland.

Table 4-3: Top 10 sites which have seen more frequent flood more than 10-year return period flood. multiple sites have equal event counts at the lower ranks, for summary purposes subset (Top 10) is shown here, while the full list of sites and event frequencies is available in the appendices.

Station ID	NZ Segments	Station Name	Number of Events	Type	Event Dates
3819	1023766	Waiharakeke at Willowbank	10	2	1968-04-04, 1971-08-04, 1971-08-05, 1988-03-11, 2002-06-21, 2011-01-29, 2014-07-10, 2014-07-11, 2014-07-12, 2020-07-18
46632	1033900	Whakapara at Cableway	10	2	1969-02-15, 1973-07-17, 1976-01-14, 1976-09-06, 1976-09-07, 1989-01-06, 2011-01-29, 2018-06-21, 2020-07-18, 2023-02-13
46651	1053888	Manganui at Permanent Station	10	3	1960-06-26, 1960-07-01, 1960-07-02, 1960-07-03, 1960-07-04, 1976-01-14, 1976-01-15, 2007-07-11, 2023-02-14, 2023-02-15
46644	1040112	Wairua at Purua	9	2	1978-06-18, 1988-03-08, 1988-03-09, 1989-01-07, 1989-01-08, 1989-09-08, 1995-03-30, 2020-07-18, 2023-02-14
1316	1006428	Awanui at School Cut	8	3	1958-02-24, 1998-08-27, 2002-06-21, 2003-03-28, 2004-02-29, 2020-07-18, 2022-08-18, 2022-08-19
47804	1015214	Waipapa at Forest Ranger	8	2	1980-02-14, 1997-09-09, 2001-12-02, 2007-02-07, 2007-03-29, 2007-07-10, 2008-02-23, 2022-08-18
1046651	1037586	Opouteke at Suspension Br	8	2	1984-12-15, 1985-02-16, 1986-01-25, 1988-03-07, 2001-12-02, 2007-07-10, 2023-02-13, 2023-02-14
802	1003880	Selwyn Swamp at Big Flat Rd	7	3	1969-06-15, 1972-11-20, 1999-04-26, 2000-06-28, 2003-05-02, 2023-05-04, 2023-05-05
4901	1041091	Ngunguru at Dugmores Rock	7	3	1975-06-14, 1977-07-20, 2000-06-29, 2000-12-11, 2007-03-29, 2011-01-29, 2012-03-19
6018	1055884	Ahuroa at Braigh	7	1	1997-06-30, 1998-07-26, 2005-07-06, 2006-08-06, 2011-01-29, 2023-02-13, 2023-02-14

Figure 4-1 shows four large events and their spatial spread. In general, it is interesting to note that summers events are mostly occurring at the lower part of Northland and winter floods are occurring mostly in the upper part of Northland.

Several limitations should be considered when interpreting the results of this analysis. Firstly, the identification and spatial extent of widespread events are inherently constrained by the availability and distribution of the flow monitoring network at the time of each event. In earlier decades, network density was limited and operational periods were shorter, resulting in low proportions of the total potential network being available during many events. As a consequence, the spatial extent of historical events is likely to be underestimated, and apparent temporal changes in event coverage may partly reflect improvements in monitoring infrastructure rather than changes in hydro-climatic behaviour.

Secondly, event coverage was assessed using a binary availability criterion (site operational or not) and did not explicitly account for data quality issues beyond station start and end dates. Periods of partial record loss, rating curve uncertainty during high flows, or short-duration data gaps may influence whether an event is detected at a given site. While the use of both mean and median statistics reduces sensitivity to individual high-coverage events, some bias associated with uneven data completeness is unavoidable.

Finally, the analysis treats all sites equally, regardless of catchment size, hydrological regime, or spatial proximity. As a result, the coverage metric reflects the proportion of gauges responding, rather than the proportion of total catchment area affected. This approach is appropriate for assessing network-wide coherence but may not fully represent the physical footprint of individual events. These limitations should be considered when using the results for long-term trend assessment or comparative analysis across periods with substantially different monitoring capability.

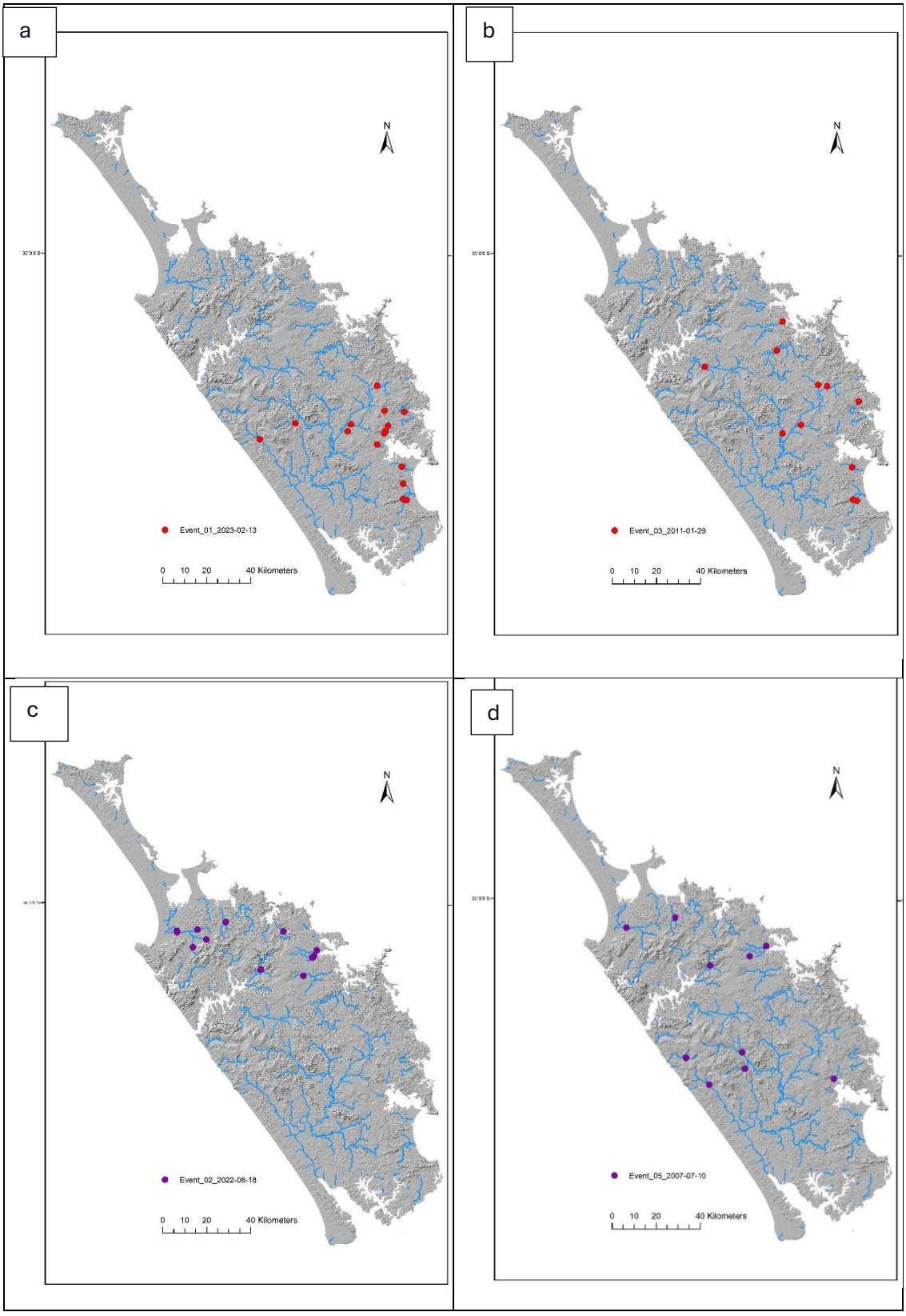


Figure 4-1: Four large events and spatial distribution of events.

4.3 Storm analysis

For each widespread event listed in Appendix B, integrated vapour transport (IVT) fields were examined for the 72-hour period preceding the event date to characterise the large-scale atmospheric conditions associated with extreme flows. This analysis provides insight into the storm-scale moisture transport mechanisms that contributed to the generation of spatially coherent hydrological responses across the monitoring network.

The IVT analysis highlights the role of sustained moisture advection in preconditioning catchments and driving high-magnitude runoff responses. In many cases, events were associated with prolonged periods of enhanced IVT directed toward the region, indicative of organised synoptic systems capable of delivering large volumes of moisture over relatively broad spatial scales. These conditions are consistent with storm types known to produce widespread flooding, including strong frontal systems and atmospheric river–like features.

Across the broader event set, similar IVT patterns were commonly observed prior to the largest and most spatially extensive events, reinforcing the link between persistent moisture transport and widespread hydrological extremes. These findings are consistent with the seasonal dominance of winter events identified earlier and underscore the importance of synoptic-scale processes in controlling the timing and extent of extreme flows.

As an illustrative example, the event of 18 August 2022 (Figure 4-1c) was preceded by a period of elevated IVT persisting for a few days prior to the peak flows. The corresponding IVT fields (Figure 4-2) show a well-defined moisture transport corridor impinging on the region, suggesting that sustained moisture supply played a key role in generating the observed multi-site exceedances. The alignment between elevated IVT and widespread flow responses indicates that this event was driven by large-scale atmospheric forcing rather than localised convective rainfall. We note that, for some events (e.g., 18 August 2022), the objective storm classification may differ from process-based interpretation based on IVT diagnostics, reflecting mixed or transitional storm characteristics.

The sequence of ERA5 IVT fields associated with the 18 August 2022 event shows a persistent and well-organised moisture transport signal impacting northern New Zealand over an extended period leading up to the observed widespread flow exceedances. Across the 24-hour window illustrated (Figure 4-3), a narrow corridor of enhanced IVT is consistently evident to the east of the country, with magnitudes exceeding approximately 800–1200 kg m^{-1} s^{-1}, indicating a strong and sustained moisture flux directed toward the region.

The IVT vectors indicate predominantly north to north-easterly moisture transport, with only minor temporal variation in orientation, suggesting that the large-scale circulation remained relatively stationary during the period of interest. This persistence implies continuous moisture supply rather than a short-lived frontal passage, increasing the likelihood of cumulative rainfall and progressive catchment wetting. The spatial coherence of the IVT signal, extending over several degrees of latitude, is consistent with synoptic-scale forcing rather than localised convective processes.

Notably, elevated IVT values are already well established by the early hours of 18 August and remain present throughout the day, indicating that catchments were likely subject to prolonged moisture loading prior to peak flows. This temporal persistence aligns with the widespread nature of the observed hydrological response, with multiple sites exceeding the 10-year return

period threshold on the same date (Fig 4-1c). The sustained IVT signal suggests that antecedent conditions, including soil moisture preconditioning, likely played an important role in amplifying runoff responses across the network.

While the IVT corridor does not appear to undergo rapid intensification immediately prior to the event, its longevity and focused structure are characteristic of storm systems capable of producing regionally extensive impacts. The absence of strong directional shifts further supports the interpretation that the event was driven by a stable synoptic pattern delivering continuous moisture, rather than by rapidly evolving or transient atmospheric features.

Overall, the IVT analysis for this event demonstrates a clear link between persistent large-scale moisture transport and spatially coherent extreme flow responses, reinforcing the broader finding that widespread hydrological events in the region are closely associated with sustained synoptic forcing rather than short-duration, localised rainfall extremes.

The IVT fields associated with the 29 January 2011 summer event display a markedly different atmospheric structure compared with the winter event of 18 August 2022. While locally elevated IVT values are evident near northern New Zealand at several time steps, the moisture transport signal is less persistent and less spatially coherent over the broader domain. Enhanced IVT appears primarily confined to a relatively narrow region east and north-east of the country and exhibits greater temporal variability in both magnitude and orientation across the 24-hour period shown in Figure 4-3.

In contrast to the sustained north-easterly moisture corridor observed during the August 2022 event, the January 2011 IVT vectors indicate more variable flow directions, with alternating north-easterly and easterly components and a greater influence of zonal flow to the south. Periods of elevated IVT are evident at individual time steps, particularly during the early morning and evening hours, but these do not persist continuously throughout the day. This intermittency suggests that moisture delivery was episodic rather than sustained, reducing the potential for prolonged catchment wetting.

Additionally, although peak IVT magnitudes locally approach values comparable to those observed in the winter case, the spatial footprint of high IVT is more limited, and the broader regional moisture transport signal is weaker. The absence of a long, well-defined moisture transport corridor impinging on the region indicates that this event was likely driven by shorter-lived atmospheric features rather than by stable synoptic-scale forcing.

These characteristics are broadly consistent with a summer-type event, in which runoff generation is driven primarily by short-duration, high-intensity rainfall and more localised forcing acting on comparatively drier antecedent conditions. In this context, *spatial coherence* refers to the degree to which neighbouring sites respond concurrently. While the total number of responding sites is not substantially lower than for the winter event, site responses during the summer event are more heterogeneous in space, with some nearby sites exhibiting high flows while others do not. This contrasts with the winter event, where sustained moisture transport and wet antecedent conditions resulted in more spatially contiguous and synchronous exceedances across the monitoring network.

These examples show that spatially extensive floods depend not only on IVT magnitude, but also on its persistence, directional stability, and spatial coherence., which are more commonly observed during winter storm regimes.

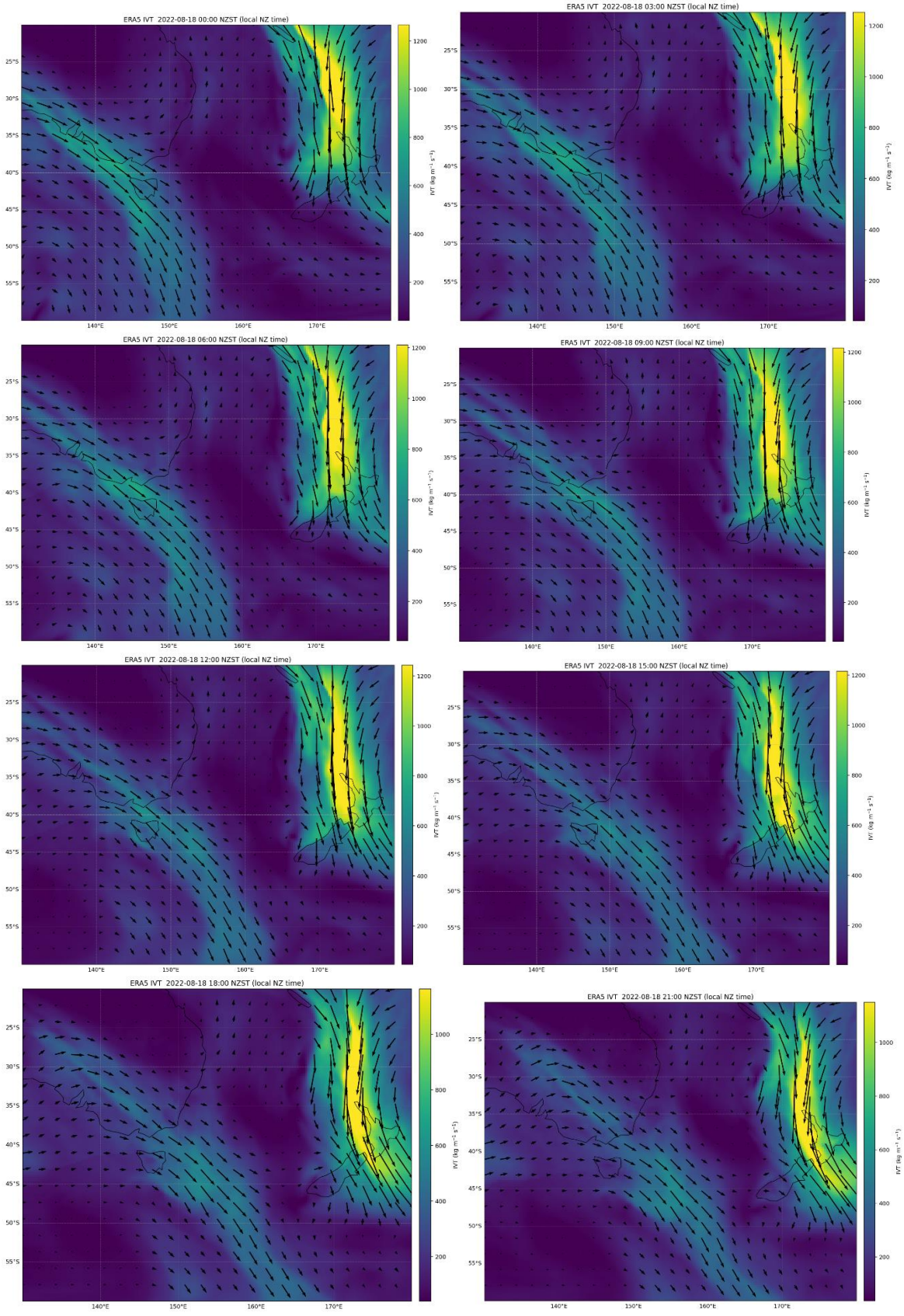


Figure 4-2: ERA5 integrated vapour transport (IVT) fields for the 18 August 2022 winter event at 3-hourly intervals (NZST),illustrating sustained and spatially coherent moisture transport affecting northern New Zealand.

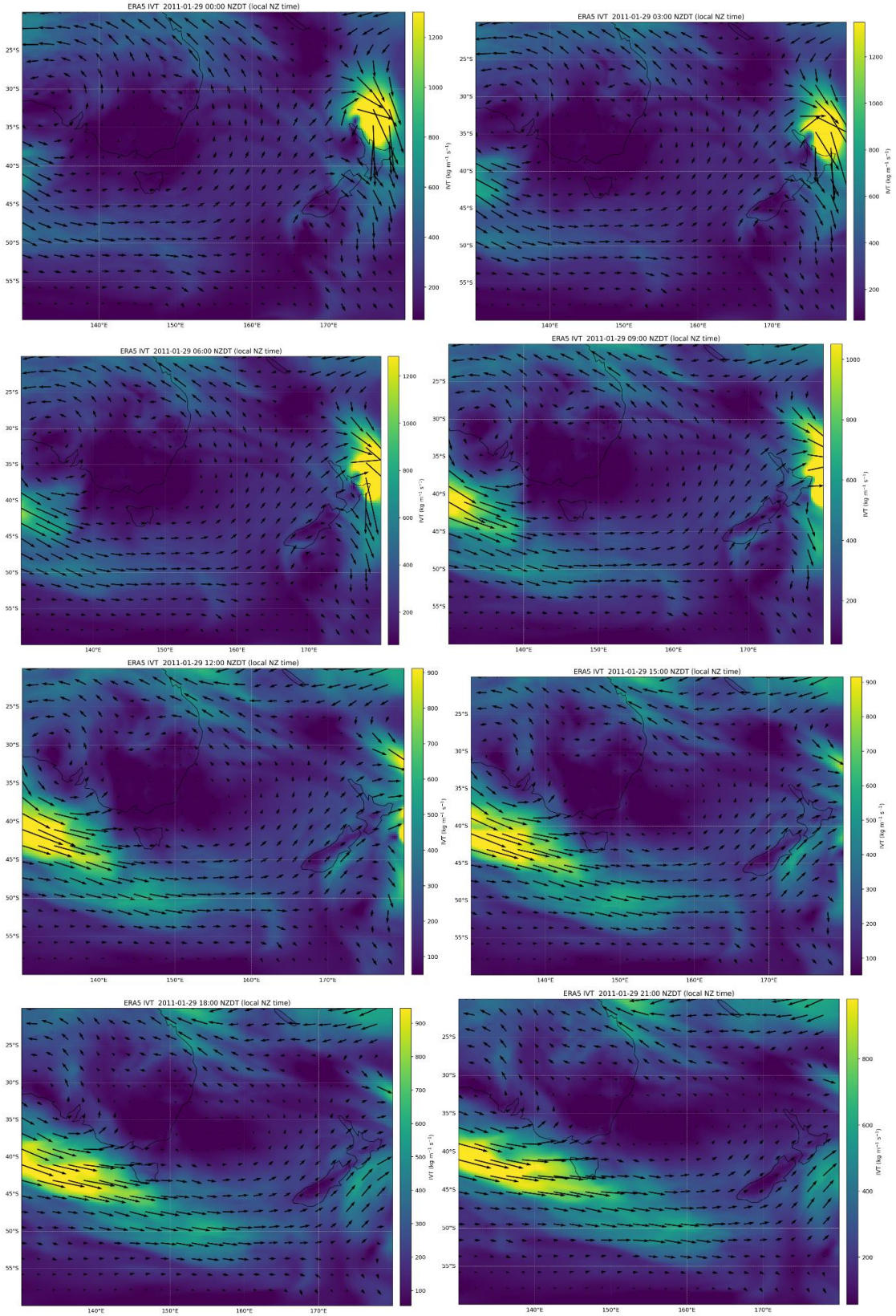


Figure 4-3: ERA5 integrated vapour transport (IVT) fields for the 29 January 2011 summer event at 3-hourly intervals (NZDT). Illustrating episodic and spatially confined moisture transport affecting northern New Zealand.

4.4 Integrated Analysis of Classified Flood Types and Event Characteristics

4.4.1 Classification and frequency of flood hydrograph types

Flood events across the study region were classified into three distinct hydrograph types based on their temporal discharge response. In total, 65 sites were analysed. The distribution of flood hydrograph types shows clear dominance of Type 2 events, followed by Type 3 and Type 1 (Table 4-4).

- Type 1 flood hydrographs were identified at 16 sites, representing 24.6% of all sites.
- Type 2 flood hydrographs were the most prevalent, occurring at 28 sites (43.1%).
- Type 3 flood hydrographs were observed at 21 sites, accounting for 32.3% of the total.

This distribution indicates that nearly three-quarters of sites exhibit either Type 2 or Type 3 flood behaviour, highlighting the predominance of relatively strong and sustained flood responses across the region.

Table 4-4: The table summarises the number of monitoring sites classified into each flood hydrograph type.

Flood hydrograph Type	Number of sites	Percentage of total sites (%)
1	16	24.6
2	28	43.1
3	21	32.3

4.4.2 Characteristics of representative flood hydrographs

Representative flood events for each hydrograph type reveal systematic differences in rise time, peak magnitude, and recession behaviour (Figure 4-4 and Figure 4-5).

Type 1 hydrographs display a short response duration, with a rapid rise to a relatively modest peak followed by a quick recession. The representative Type 1 event reaches its peak within approximately 2–3 days and returns to near-baseflow conditions shortly thereafter. This response suggests a limited storage effect and relatively small contributing catchment or efficient drainage pathways.

In contrast, Type 2 hydrographs are characterised by a sharp and pronounced peak, with a rapid rising limb followed by a longer recession. The representative Type 2 event reaches peak discharge early in the event, indicating a strong catchment response to rainfall, while the extended recession implies the contribution of delayed flow components such as shallow subsurface flow or floodplain storage.

Type 3 hydrographs show the longest duration and most sustained flow response. The representative event exhibits a more gradual rise to peak discharge and a slow recession that extends over several days. Peak flows are comparable to or higher than those observed in Type 2 events, but the distinguishing feature of Type 3 floods is their prolonged elevated discharge, indicating substantial catchment storage and delayed drainage mechanisms.

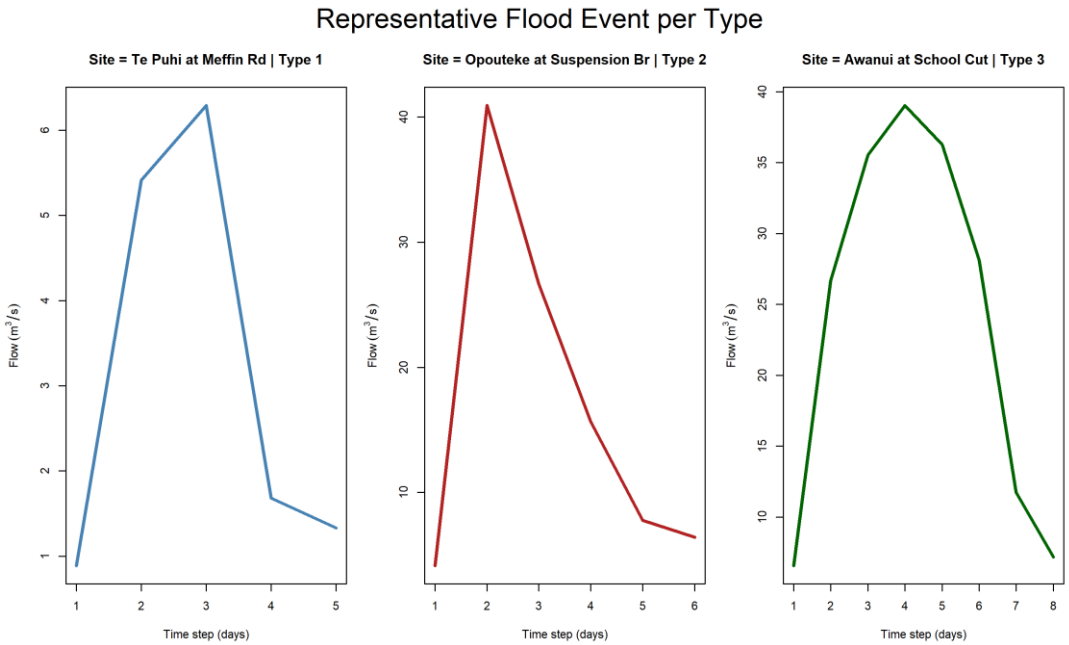


Figure 4-4: Representative flood hydrographs for the three flood hydrograph types.

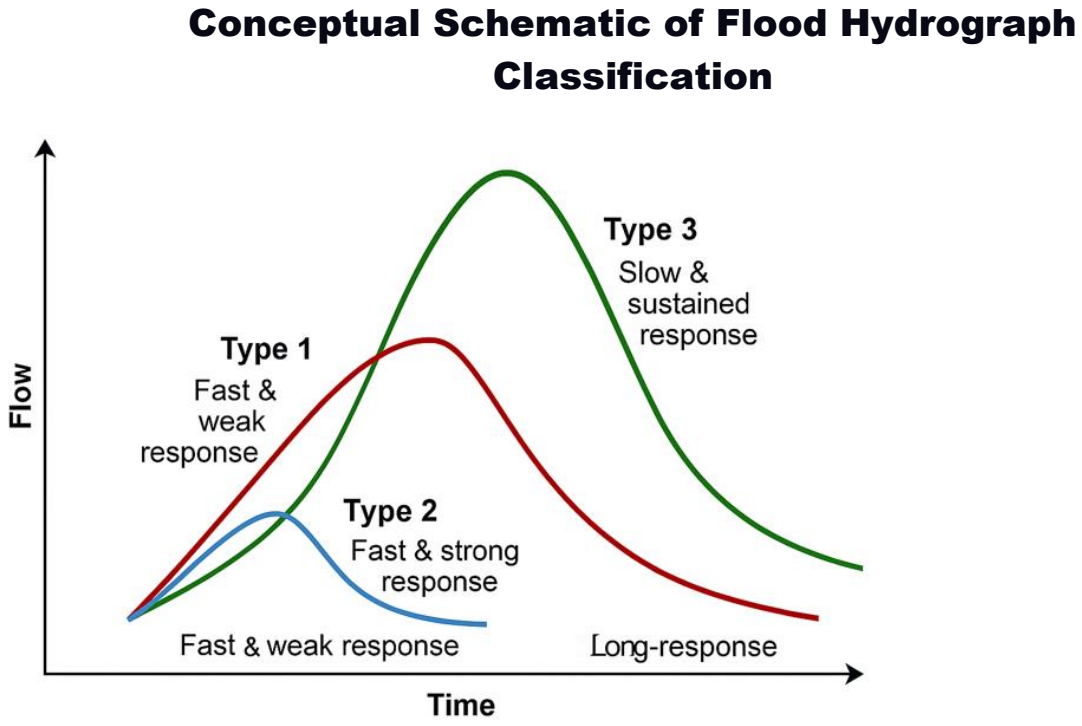


Figure 4-5: Conceptual schematic of flood hydrograph classification and catchment response behaviour.

4.4.3 Spatial distribution of flood hydrograph types

The spatial distribution of the three flood hydrograph types across the study area is shown in Figure 4-6. Type 1 sites are sparsely distributed and tend to occur in smaller catchments, suggesting specific hydrological or geomorphological controls. Type 2 sites are widely distributed throughout the region and form the dominant pattern, indicating that fast-responding catchments with pronounced flood peaks are common across diverse physiographic settings.

Type 3 hydrographs, while less frequent than Type 2, show distinct spatial clustering in certain parts of the region. These clusters suggest areas where catchment properties promote prolonged flood responses, potentially associated with larger drainage areas, flatter valley bottoms, or greater floodplain connectivity.

The observed flood hydrograph types reflect differences in catchment response mechanisms, including runoff generation, storage, and drainage efficiency. Type 1 floods likely correspond to smaller or steeper catchments where rainfall is rapidly converted to runoff but with limited water storage, resulting in brief flood events with low attenuation. Such responses are typical of catchments dominated by shallow soils or efficient surface drainage networks.

Type 2 floods, which represent the largest proportion of sites, indicate catchments with high runoff efficiency but also sufficient subsurface or channel storage to sustain elevated flows beyond the peak. The sharp rising limb suggests rapid runoff generation, while the moderate recession reflects delayed contributions from storage components. The dominance of Type 2 behaviour implies that much of the region responds quickly to storm events while still exhibiting some buffering capacity.

Type 3 floods represent the most prolonged and potentially hazardous flood responses. The gradual rise and long recession are consistent with catchments that have substantial storage, such as larger basin areas, extensive floodplains, wetlands, or permeable subsurface layers that release water slowly. Although Type 3 floods are less frequent than Type 2, their extended duration may result in greater cumulative impacts, including prolonged inundation and higher flood volumes.

The predominance of Type 2 and Type 3 flood behaviour (75.4%) has important implications for flood risk management in the region. While Type 2 floods pose an immediate hazard due to sharp peak discharges, Type 3 floods present a different but equally significant risk through sustained high flows and prolonged inundation periods.

The spatial distribution of flood types indicates that Type 3 responses tend to cluster in upstream or low-gradient reaches where storage effects and catchment wetness promote prolonged runoff generation. In contrast, some downstream locations exhibit Type 2 behaviour despite receiving flow from Type 3 upstream sites, suggesting attenuation and transformation of the flood hydrograph along the river network. In such cases, prolonged upstream inflows may translate downstream into sharper peaks due to channel routing effects, confluences with fast-responding tributaries, or reduced floodplain storage.

These patterns indicate that flood mitigation strategies should consider longitudinal variability in flood behaviour. Upstream areas prone to Type 3 flooding may benefit from measures addressing extended inundation and cumulative impacts, whereas downstream reaches dominated by Type 2 responses may require early warning systems and preparedness strategies focused on rapid flood onset.

Overall, the classification of flood hydrograph types provides a useful framework for understanding regional flood dynamics. By linking hydrograph shape, frequency, and spatial distribution, this analysis highlights the diversity of flood responses across the study area and underscores the need for flood management approaches that are tailored to dominant catchment-scale hydrological behaviour.

Figure 4-7 shows the annual number of events exceeding the 10-year return period. No clear temporal pattern is evident from the figure.

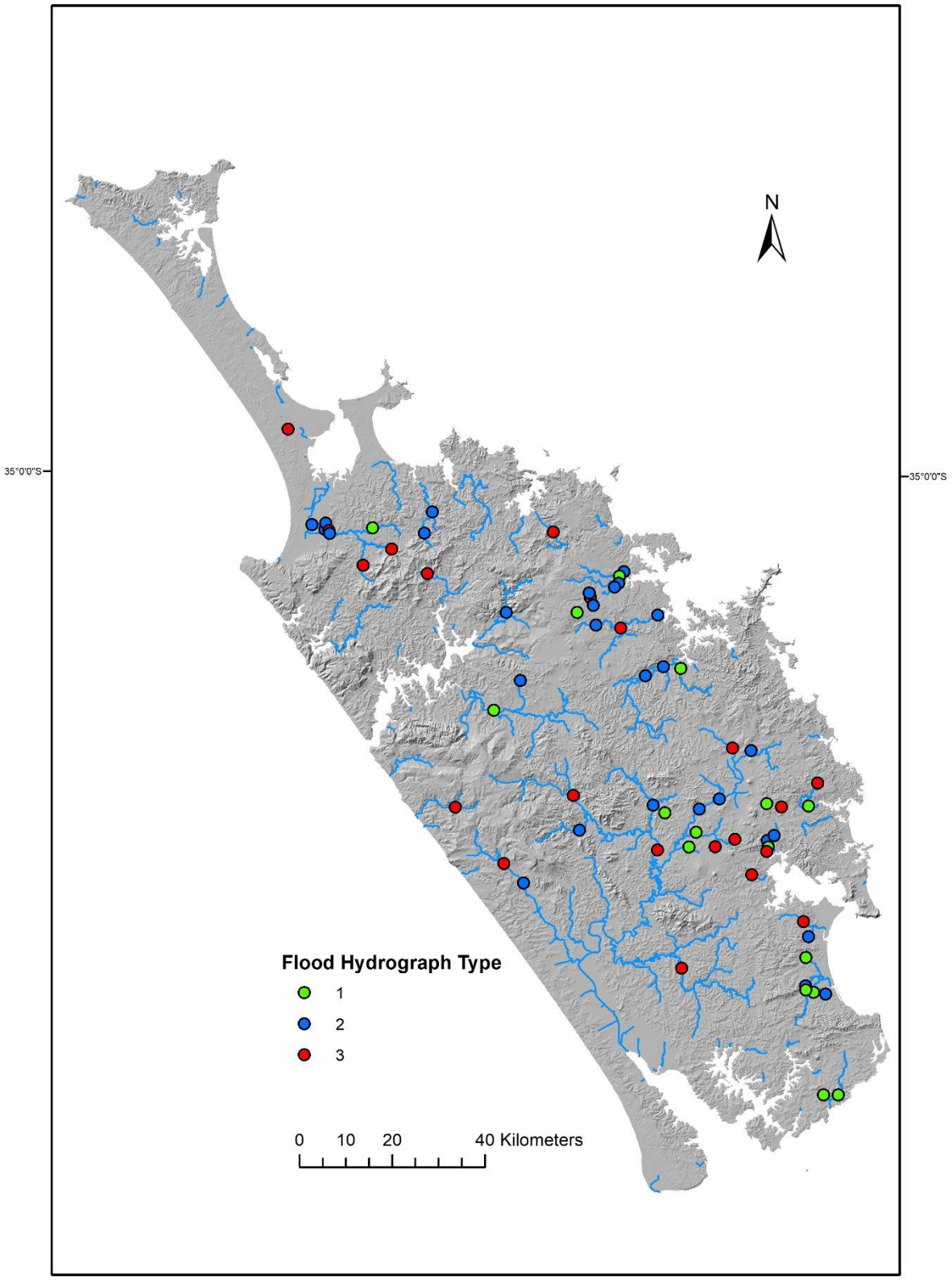


Figure 4-6: Spatial distribution of flood hydrograph types across the study area.

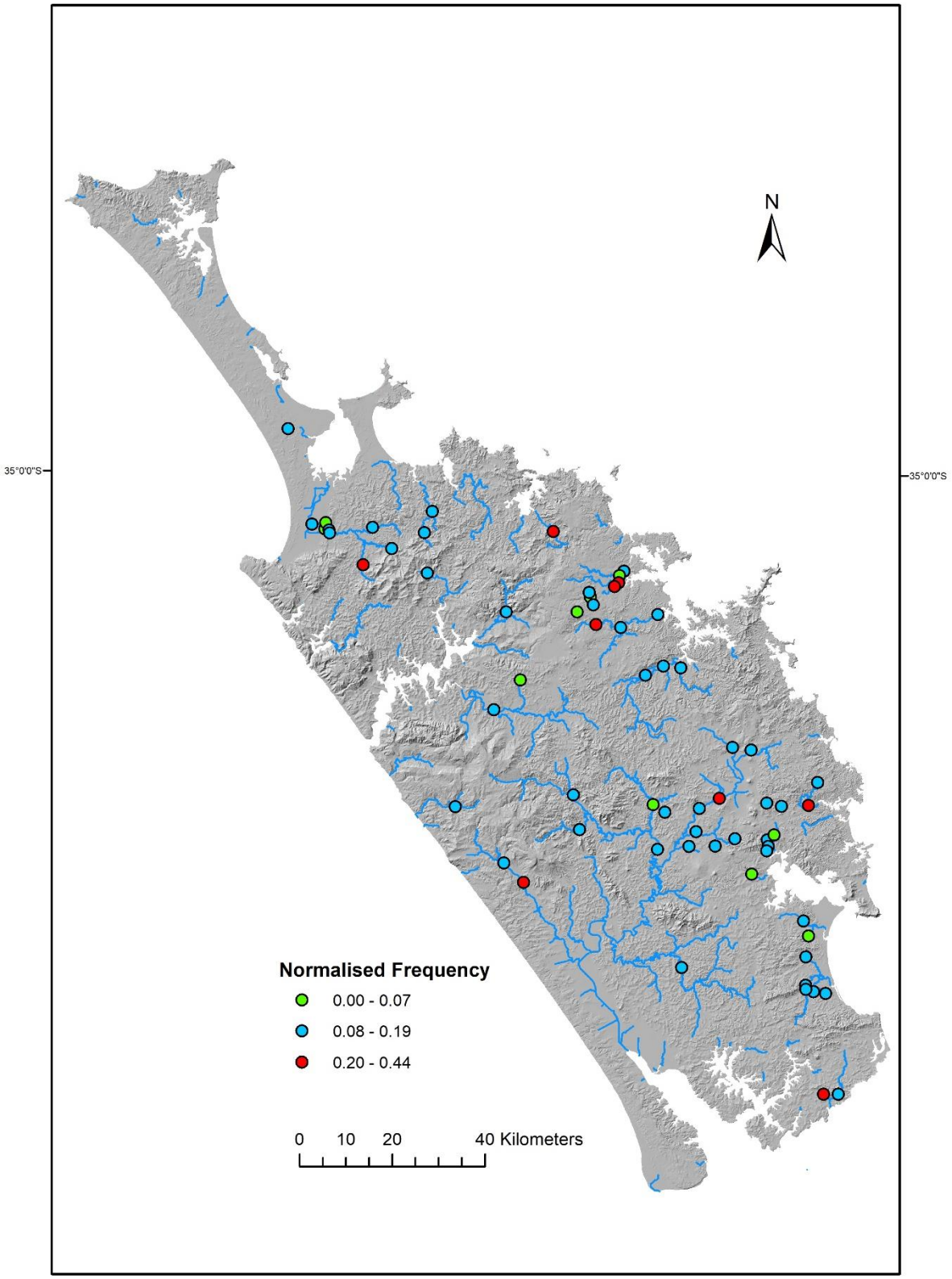


Figure 4-7: Spatial distribution of normalised flood frequency. Number of flood events per year across the study area.

4.4.4 Climate controls on flood hydrograph types

The spatial distribution and relative frequency of the three flood hydrograph types indicate that both site-specific catchment characteristics and event-scale atmospheric forcing influence flood response. The clear spatial clustering of hydrograph types suggests that location and by extension catchment properties such as size, slope, drainage efficiency, storage capacity, and connectivity may be associated with the predominant flood response at a given site.

Type 1 flood hydrographs, which account for 24.6% of sites, are predominantly observed at locations that consistently exhibit short-duration, low-volume responses. These sites are most responsive to short-duration, high-intensity convective rainfall or localised convective storm, which produce rapid runoff generation but limited catchment wetting, resulting in brief flood events with minimal sustained runoff.

Type 2 hydrographs, the dominant class (43.1% of sites), tend to occur at sites where catchment characteristics support rapid runoff generation while still allowing for moderate storage and attenuation. These sites frequently respond to widespread frontal systems or moderate-duration storm events, producing sharp rising limbs followed by extended recessions associated with subsurface contributions and channel routing. The prevalence of Type 2 behaviour suggests that many catchments in the region are may be inclined toward this intermediate response across a wide range of event types.

Type 3 hydrographs (32.3% of sites) are spatially clustered at locations that favour prolonged flood responses, reflecting large contributing areas, low gradients, or significant floodplain and subsurface storage. At these sites, long-duration rainfall associated with slow-moving frontal systems, atmospheric rivers, or multi-day storm sequences can amplify this inherent tendency, leading to progressive soil saturation, increased catchment connectivity, sustained elevated flows, and extended recession limbs.

Together, these patterns indicate that site characteristics appear to strongly influence the dominant hydrograph type , while storm type controls the likelihood and severity of that response during individual events, occasionally overriding typical behaviour under extreme forcing.

4.4.5 Influence of land use and catchment characteristics

Land use and catchment characteristics play a critical role in modulating how climatic inputs translate into flood hydrograph shape. Type 1 flood responses are most consistent with small, steep or well-drained catchments, potentially located in upper headwaters or areas with limited storage capacity. In such settings, rainfall is rapidly conveyed to the channel network with little delay or attenuation, causing brief flood pulses.

The widespread occurrence of Type 2 floods across the study area suggests the presence of catchments that combine efficient runoff generation with moderate storage capacity. These characteristics are typical of mixed land-use basins where pastoral or agricultural land dominates, often with modified drainage networks that enhance surface runoff while retaining some subsurface flow pathways. Channel geometry and floodplain connectivity likely play an important role in extending the recession phase for these sites.

Type 3 flood hydrographs are indicative of catchments with substantial hydrological storage, such as larger basin areas, low-gradient floodplains, wetlands, or permeable geologic units. The

spatial clustering of Type 3 sites suggests that land-use patterns combined with topography amplify the effects of prolonged rainfall, allowing water to be stored and slowly released over several days. These areas are particularly vulnerable to long-duration flooding, which may produce greater cumulative impacts despite not always generating the sharpest flood peaks.

4.4.6 Implications under current and future climatic conditions

The dominance of Type 2 and Type 3 flood responses (75.4%) indicates that the region is particularly sensitive to storms capable of generating either high peak flows or prolonged wet periods. Under projected climate change scenarios, which suggest increases in extreme rainfall intensity and longer-duration storm events (Rosier et al, 2024), the frequency and severity of Type 2 and Type 3 floods may increase.

Type 2 floods may become more hazardous due to enhanced peak discharges, increasing the risk of flash flooding and infrastructure failure. Meanwhile, Type 3 floods may pose growing challenges for flood management due to extended inundation durations, which can exacerbate erosion, landslide risk, and prolonged disruption to communities and land use.

Overall, the integration of flood hydrograph classification with spatial analysis provides valuable insight into how climate drivers and land-use characteristics interact to shape regional flood behaviour. This framework offers a useful basis for developing flood risk mitigation strategies that are sensitive to both dominant flood mechanisms and local catchment controls.

4.5 Influence of ENSO and SAM on flood behaviour

The following definitions were used for the spatial spread of events:

- Widespread ≈ large, spatially coherent events (n_sites ≥ ~8)
- Moderate spread ≈ moderate regional events (4 ≤ n_sites < 8)
- Localised ≈ localised events (n_sites ≤ 3)

The identified events with ENSO and SAM index are given in Appendix C. Analysis of regional flood events suggests a potential influence of large-scale climate modes on flood behaviour (Table 4-5). However, these results are based on simple frequency counts and have not been normalised by the relative occurrence of ENSO and SAM phases. Therefore, the observed differences should be interpreted as indicative rather than statistically robust relationships. Widespread events appear to occur more frequently during La Niña and Neutral conditions; however, this pattern may partly reflect differences in the frequency of ENSO phases and should be interpreted with caution. Similarly, localised flood events are more commonly observed during Neutral ENSO conditions, although the strength of this relationship cannot be confirmed without further statistical analysis.

The Southern Annular Mode (SAM) may also influence flood characteristics, although the strength of this relationship cannot be confirmed without formal statistical testing (Table 4-6). Positive SAM phases, characterised by a poleward shift of the Southern Hemisphere westerlies and enhanced subtropical moisture transport toward northern New Zealand, are associated with wetter and more persistent rainfall conditions. In this context, the observed prevalence of Type 3 flooding during positive SAM phases is consistent with hydrological responses driven by

sustained rainfall and elevated antecedent wetness. Negative SAM phases, by contrast, are more commonly associated with shorter-duration or more spatially heterogeneous events.

Storm classification using NIWA's multi-hazards archive confirms that Northland's most severe floods are overwhelmingly associated with extra-tropical cyclones, often enhanced by persistent atmospheric rivers. Events such as March 2007, July 2007, July 2020, January 2011 (Cyclone Wilma), and February 2023 (Cyclone Gabrielle) exhibit consistent characteristics: long rainfall duration, strong moisture transport from the subtropics, basin-filling river responses, and widespread impacts across multiple catchments.

In contrast, events classified as localised convective storms are generally associated with localised flood responses, confined spatial extent, and short hydrological response times. These events pose different operational challenges, particularly in small or coastal catchments, but contribute less to region-wide flood risk compared to cyclone-driven systems.

The results demonstrate that flood hazard in Northland is not solely a function of rainfall intensity, but strongly dependent on storm persistence, moisture transport pathways, and large-scale atmospheric state. ENSO and SAM do not directly cause flooding but instead tilt the probability toward storm types capable of producing widespread or localised flood impacts.

The integration of storm typology with climate phase information provides a practical foundation for phase-aware flood preparedness. For example, La Niña conditions combined with positive SAM substantially increase the likelihood of ETC-AR events, supporting early escalation of preparedness, staffing, and inter-agency coordination. Conversely, neutral ENSO periods may warrant heightened vigilance for short-duration convective flooding, particularly in small or urban catchments.

No formal statistical significance testing (e.g. chi-square or contingency table analysis) was undertaken to assess whether the observed relationships are significantly different from random variation. A more rigorous assessment, including normalisation by the frequency of ENSO and SAM phases, is recommended for future work.

Overall, the storm–flood–climate framework developed in this study provides Northland Regional Council with a transferable, evidence-informed tool for interpreting flood risk, improving post-event consistency, and supporting climate-informed operational decision-making.

Table 4-5: Distribution of flood spread by ENSO phase for identified flood events in Northland.

Flood spread	ENSO phase	Number of events
Wide spread	LaNina	3
Wide spread	Neutral	4
localised	ElNino	12
localised	LaNina	47
localised	Neutral	48
moderate spread	ElNino	2
moderate spread	LaNina	2
moderate spread	Neutral	3

Table 4-6: Distribution of flood spread by SAM phase for identified flood events in Northland.

Flood spread	SAM phase	Number of Events
Wide spread	Negative	3
Wide spread	Neutral	4
localised	Negative	42
localised	Neutral	35
localised	Positive	30
moderate spread	Negative	2
moderate spread	Neutral	4
moderate spread	Positive	1

4.6 Operational implications for NRC

Figure 4-8 presents a two-tier decision-support framework that links meteorological storm type to expected flood hydrograph behaviour and indicative NRC response levels. The upper tier classifies storm systems by dominant atmospheric trigger, distinguishing between atmospheric-river-assisted extra-tropical cyclones, extra-tropical cyclones without sustained moisture corridors, and localised convective outbreaks. The intermediate tier translates these storm classes into expected flood characteristics, ranging from widespread, long-duration flooding to rapid-onset, short-lag events. The lower tier maps these flood behaviours to the hydrograph types identified in this study (Type 3, Type 2, and Type 1) and indicative operational responses. This framework is intended to support rapid interpretation of forecast storm information and to assist NRC in anticipating the scale, duration, and coordination requirements of flood response.

Table 4-7 summarises the practical application of knowledge gained from this study for flood management purposes. The table translates the storm–flood classification framework into an operational decision-support process aligned with Northland Regional Council (NRC) flood preparedness, response, and post-event review activities.

At the forecast stage, NRC can monitor each event and identify the dominant storm type and the persistence of large-scale moisture transport, including the presence and strength of Integrated Vapour Transport (IVT). Based on this information, the likely flood response type (Type 1, Type 2, or Type 3) can be inferred using the classification framework, enabling early scaling of staffing, communications, and inter-team coordination.

During an event, the inferred flood type can be confirmed or refined using real-time observations of river hydrograph behaviour. Where rainfall persistence or catchment response exceeds initial expectations, operational response can be escalated, for example from a Type 2 to a Type 3 response, to reflect increasing flood duration, spatial extent, or coordination requirements.

Following the event, the same framework can be applied to classify the event retrospectively, supporting consistent post-event reporting, review, and learning across the monitoring network. This approach enables improved comparability between events and supports incremental refinement of operational thresholds and preparedness strategies over time.

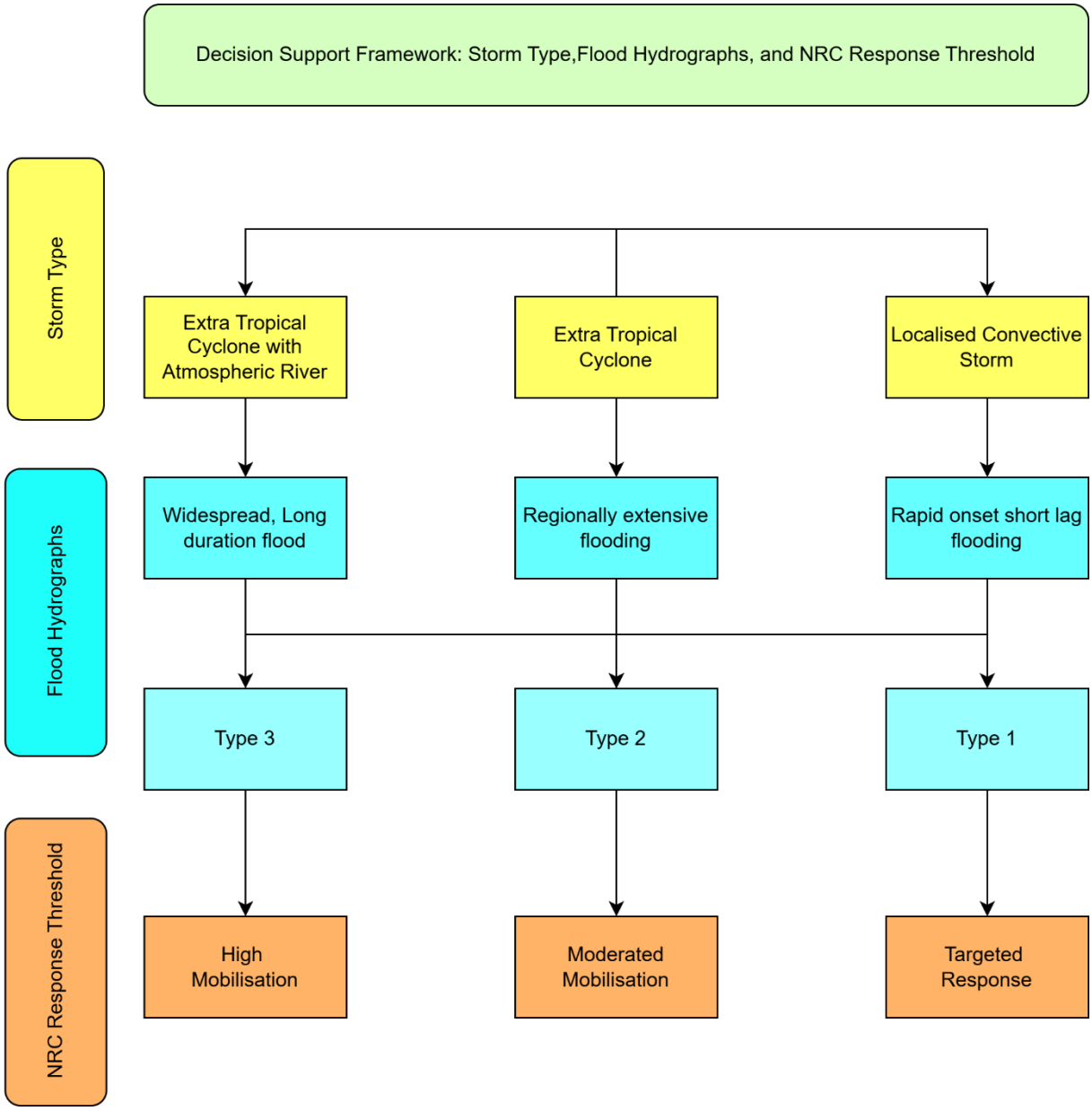


Figure 4-8: Decision-support framework linking storm type to expected flood characteristics in Northland.

Table 4-7: Decision-support table linking storm type, flood type, and NRC operational response.

Storm type	Dominant atmospheric indicators	Expected flood hydrograph type	Flood characteristics	Indicative NRC response focus
ETC with Atmospheric River	Persistent IVT ≥ 250–400 kg m^{-1} s^{-1}; strong NE–E moisture corridor; slow-moving synoptic system	Type 3	Widespread, long-duration flooding; multi-day elevated flows; slow recession; high flood volumes	High mobilisation: multi-catchment coordination; sustained staffing; floodplain and lifeline protection; prolonged response and recovery planning
Extra-tropical Cyclone (non-AR dominated)	Strong pressure gradients; frontal rainbands; moderate IVT persistence	Type 2	Regionally extensive flooding; sharp peaks with moderate recession; multi-catchment impacts	Moderate mobilisation: regional coordination; readiness for escalation; targeted asset protection
North Tasman Low / Frontal system	Slow-moving rainbands; orographic enhancement; moderate rainfall duration	Type 2	Basin-filling floods; moderate lag times; extended but manageable durations	Moderate mobilisation: monitor multiple catchments; coordinate across river groups
Localised convective storm / squall line	Radar-identified back-building cells; rainfall ≥ 40–60 mm h^{-1}; short duration	Type 1	Rapid-onset, short-lag flooding; localised impacts; steep rising limbs	Targeted response: rapid warnings; localised deployment; urban and small-catchment focus
Mixed / compound events/ High storm-tide; elevated antecedent wetness	AR + ETC or rainfall plus tide; elevated antecedent wetness	Type 2–3	Elevated risk of compound flooding; slower drainage; extended impacts	Escalated readiness: cross-team coordination; tide and drainage monitoring

5 Recommendations for future work

The findings of this study provide a robust regional framework for understanding storm flood connectivity and flood response types across Northland. Several opportunities exist to further extend and refine this work to support operational decision-making, risk assessment, and long-term planning.

- Enhanced spatial representation of rainfall forcing
  Future analyses could improve representation of rainfall variability within catchments by integrating radar-derived rainfall estimates and satellite products alongside gauge observations. Blending gauge, radar, and satellite datasets would better capture spatially heterogeneous rainfall, particularly for localised convective events and complex topography, and improve attribution of flood response to rainfall intensity and distribution.

- Ungauged Locations
  This study focused on flow gauged locations, where observed discharge data allow robust characterisation of flood behaviour. Extending the framework to ungauged catchments would substantially increase its utility for flood management in Northland. Applying regionalisation and catchment-similarity approaches would enable flood response characteristics to be inferred at data-sparse locations, improving spatial coverage of flood risk assessment. Such an extension is particularly important for small headwater and coastal catchments, enhancing preparedness, warning capability, and long-term planning across the wider river network.

- Sub-daily flood response analysis
  While daily data are appropriate for regional-scale and long-duration events, future work could incorporate sub-daily rainfall and flow data where available to better characterise short-lag and flash-flood responses. This would enable improved assessment of peak timing, rise rates, and compound hazards in small or urbanised catchments and support refinement of flood type classification for high-impact short-duration events.

- Integration of antecedent catchment conditions
  Explicit incorporation of antecedent soil moisture, groundwater level proxies, or catchment wetness indices would strengthen interpretation of event-to-event variability in flood response. Including these factors would help distinguish between rainfall-driven and storage-controlled flood behaviour and improve predictive capability under varying seasonal and climatic conditions.

- Expanded climate driver assessment
  While this study focuses on ENSO and SAM, future work could evaluate the influence of additional large-scale climate modes relevant to the southwest Pacific, such as the Interdecadal Pacific Oscillation (IPO) or regional sea-surface temperature anomalies. This would support more comprehensive climate-conditioned flood risk assessments and improve confidence in season-ahead planning and preparedness.

- Quantitative linkage to flood impacts and damages
  Further work could link classified storm and flood types to observed flood impacts, such as inundation extent, infrastructure disruption, or reported damage. This would enable prioritisation of flood mechanisms that pose the greatest risk to communities and assets and support more targeted mitigation strategies.
- Application to future climate scenarios
  The storm–flood typology developed in this study provides a strong foundation for assessing how flood behaviour may change under future climate projections. Applying the classification framework to downscaled climate model outputs would allow exploration of changes in storm frequency, storm type, and dominant flood responses, supporting climate-resilient infrastructure design and long-term regional planning.

6 Conclusions

Flood risk in Northland is strongly dependent on storm type and atmospheric forcing, with different storm mechanisms producing fundamentally different flood hazards. This study shows that atmospheric-river-assisted extratropical cyclones are the primary drivers of widespread, long-duration flooding, frequently producing record or near-record 24–48 hour cumulative discharge or sustained high-flow conditions across multiple catchments. In contrast, localised convective storms generate rapid-onset, short-lag flooding in smaller catchments, particularly in coastal and urbanised areas. These differences have direct implications for flood-warning lead times, emergency response, and infrastructure design.

Widespread flood events were most frequent during the 1960s–1980s, with approximately 21–22 events per decade. Although slightly fewer widespread events have been recorded in recent decades, several of the most extreme and high-impact floods have occurred since the 1990s, indicating that flood risk remains high and may be characterised by increasing severity rather than higher frequency.

The development of a Northland Storm–Flood Typology converts this knowledge into an operationally useful framework. By explicitly linking storm triggers, catchment response, and flood hydrograph characteristics, the typology provides NRC with a consistent basis for interpreting flood drivers, comparing events, and anticipating likely flood behaviour during future storms. The framework supports both event-specific response planning and longer-term risk management and investment decisions.

Large-scale climate variability plays an important role in shaping flood risk. The analysis indicates that ENSO and possibly the Southern Annular Mode (SAM) may influence storm frequency, atmospheric-river landfalls, rainfall persistence, and flood severity in Northland. In particular, La Niña-leaning conditions increase the likelihood of persistent moisture transport and regionally coherent flooding. Incorporating these climate-driven risk shifts into operational awareness can support phase-aware readiness, enabling NRC to adjust preparedness levels, resource deployment, and communication strategies ahead of higher-risk seasons.

The study also highlights the necessity of multi-source rainfall information for effective flood assessment and response. Rain gauges remain essential for ground truth, but on their own do not fully capture spatial rainfall variability. Radar data provide valuable spatial context within coverage limits, while satellite products such as IMERG extend visibility offshore and in data-sparse areas. Blended use of these datasets is critical for timely situational awareness during high-impact events.

At the regional scale, widespread hydrological events occur most frequently in winter, reflecting the dominance of persistent synoptic systems during this season, while spring events are relatively rare, suggesting weaker spatial coherence during transitional periods. Although monitoring network coverage during flood events has improved over time, it remains incomplete, reinforcing the need to interpret historical patterns alongside known observational limitations.

Overall, this study delivers a practical, evidence-based framework that strengthens NRC's ability to understand, anticipate, and manage flood risk across Northland. The Storm–Flood Typology provides a clear bridge between climate drivers, storm behaviour, and flood response,

supporting operational decision-making, climate-informed planning, and infrastructure resilience in an increasingly variable climate.

This study provides a transferable Storm–Flood Typology that links meteorological forcing, catchment response, and flood hazard. The framework can be applied both retrospectively for event analysis and prospectively for climate-informed flood preparedness.

7 Acknowledgements

We acknowledge the assistance of Soe Thiha of NRC staff and Charles Pearson, Ude Shankar and Kathy Walter of NIWA staff. Funding for this study was provided by Envirolink.

8 Glossary of abbreviations and terms

NRC	Northland Regional Council
ESNZ	Earth Sciences New Zealand
ENSO	El Niño–Southern Oscillation
SAM	Southern Annular Mode
IPO	Interdecadal Pacific Oscillation
IVT	Integrated Vapour Transport
NZMS	New Zealand Meteorological Service
DEM	Digital Elevation Model
REC	River Environment Classification
AR	Atmospheric River
GEV	Generalised Extreme Value distribution
IBTrACS	International Best Track Archive for Climate Stewardship

9 References

Bollinger, L., Kennedy, D. (2012) *Community resilience to hazard events*. GNS Science Report.

Chappell, P.R. (2013) *The Climate and Weather of Northland*. NIWA Science and Technology Series No. 59, 40 pp.

Comola, F., Satyam, S., Scudeler, C., Prakash, M., Uhlemann-Elmer, S., Drayton, M., Nicotina, L. (2021) Impacts of ENSO on flood risk in New Zealand. *EGU General Assembly*.

Fischer, S., Pahlow, M., Singh, S.K. (2025) Impact of catchment and climate attributes on flood generating processes and their effect on flood statistics, Journal of Hydrology, Volume 646,132361, https://doi.org/10.1016/j.jhydrol.2024.132361.

Gaume, E., et al. (2009) *A review of flash flood processes and modelling*. Journal of Hydrology, 394, 1–17.

Gray, W. (2003) *Overview of weather and coastal hazards in the Northland region – Part I: Weather hazards*. NIWA Client Report WLG2003-57.

Hersbach, H., Bell, B., Berrisford, P., Biavati, G., Horányi, A., Muñoz Sabater, J., Nicolas, J., Peubey, C., Radu, R., Rozum, I., Schepers, D., Simmons, A., Soci, C., Dee, D., and Thépaut, J.-N.: ERA5-Land hourly data from 1981 to present, Copernicus Climate Change Service (C3S) Climate Data Store (CDS) [dataset], https://doi.org/10.24381/cds.adbb2d47, 2018.

Hersbach, H., Bell, B., Berrisford, P., Hirahara, S., Horányi, A., Muñoz-Sabater, J., Nicolas, J., Peubey, C., Radu, R., Schepers, D., Simmons, A., Soci, C., Abdalla, S., Abellan, X., Balsamo, G., Bechtold, P., Biavati, G., Bidlot, J., Bonavita, M., De Chiara, G., Dahlgren, P., Dee, D., Diamantakis, M., Dragani, R., Flemming, J., Forbes, R., Fuentes, M., Geer, A., Haimberger, L., Healy, S., Hogan, R. J., Hólm, E., Janisková, M., Keeley, S., Laloyaux, P., Lopez, P., Lupu, C., Radnoti, G., de Rosnay, P., Rozum, I., Vamborg, F., Villaume, S., and Thépaut, J.-N.: The ERA5 global reanalysis, Q. J. Roy. Meteor. Soc., 146, 1999–2049, https://doi.org/10.1002/qj.3803, 2020.

Knapp, K. R., Kruk, M. C., Levinson, D. H., Diamond, H. J., & Neumann, C. J. (2010) The International Best Track Archive for Climate Stewardship (IBTrACS): Unifying tropical cyclone best track data. Bulletin of the American Meteorological Society, 91, 363–376. https://doi.org/10.1175/2009BAMS2755.1

Marshall, G. J., 2003: Trends in the Southern Annular Mode from Observations and Reanalyses. *J. Climate*, **16**, 4134–4143, https://doi.org/10.1175/1520-0442(2003)016<4134:TITSAM>2.0.CO;2.

McKerchar, A.I., Henderson, R.D. (2003) *Flooding in New Zealand: causes and characteristics*. Journal of Hydrology (NZ), 42(2), 59–72.

Merz, B., et al. (2014) *Floods and climate: emerging perspectives*. Nature Climate Change, 4, 795–805.

NIWA (2025) *Northland Regional Climatology*. NIWA Regional Climate Series.

NOAA Climate Prediction Center (CPC). Niño 3.4 Index (monthly), based on ERSSTv5. NOAA Physical Sciences Laboratory. https://psl.noaa.gov/data/timeseries/month/Nino34_CPC/

NOAA Physical Sciences Laboratory (PSL). Southern Annular Mode (SAM) Index (monthly), derived from zonal-mean sea-level pressure. https://psl.noaa.gov/data/20thC_Rean/timeseries/monthly/SAM/

Pfahl, S., Wernli, H. (2012) Quantifying the relevance of cyclones for precipitation extremes.
Journal of Climate, 25(19), 6770–6780. https://doi.org/10.1175/JCLI-D-11-00705.1

Prince, H.D., Cullen, N.J., Gibson, P.B., et al. (2021) A climatology of atmospheric rivers in New Zealand. *Journal of Climate*, 34, 4383–4402.

Revell, M.J., et al. (2016) *Atmospheric rivers and extreme rainfall over New Zealand*. Monthly Weather Review, 144, 1–18.

Rosier, S. M., Bodeker, G. E., Carey-Smith, T. K., Frame, D. J., Gibson, P. B., Harrington, L. J., Stone, D. A. (2024) Changing rainfall extremes with climate change in New Zealand: Guidance for decision-makers. Deep South National Science Challenge.

Sinclair, M.R. (2002) *Extratropical transition of southwest Pacific tropical cyclones. Part I: Climatology and composite structure*. Monthly Weather Review, 130, 590–609.

Singh, S.K., Griffiths, G.A., Pham, H.X. (2021) Meteorological drought in Northland, New Zealand. *Journal of Hydrology (NZ)*, 60(1), 1–16.

Vo, D-P., Chang, Y., Shamseldin, A. (2026) *Assessment of Cyclone Gabrielle and Mangawhai Flash Flood*. NRC.

Woods, R.A., McKerchar, A.I. (2003) *Hydrological hazards of New Zealand*. In *Natural Hazards of New Zealand*.

Zscheischler, J., et al. (2020) *Future climate risk from compound events*. Nature Climate Change, 10, 586–595.

Appendix A Descriptive statistics of sites used in this study

Site ID	Station Name	latitude	longitude	NZ Segments	Start Date	End Date	Mean Flow (m^3/s)	Median' Flow (m^3/s)	Sd Flow (m^3/s)	Cv Flow	Min Flow (m^3/s)	Max Flow (m^3/s)	Record Length (years)	Mean Annual Max (m^3/s)	Median Annual Max (m^3/s)	Max Annual Max (m^3/s)	RL 10 (m^3/s)	N Daily Exceed RL10
1046651	Opouteke at Suspension Br	-35.6957	173.8667	1037586	13/12/1984	2/10/2025	4.16	2.17	7.52	1.81	0.31	163.09	42	73.59	65.35	163.09	122.52	8
1313	Tarawhataroa at Pukepoto Rd	-35.1141	173.2576	1006404	23/09/1971	9/05/1980	0.61	0.30	1.25	2.06	0.10	27.60	10	13.22	10.08	27.60	33.38	0
1314	Awanui at Waikuruki	-35.1022	173.2593	1006270	4/04/1990	2/10/2025	5.38	3.13	6.39	1.19	0.20	56.08	36	36.03	37.87	56.08	51.54	1
1316	Awanui at School Cut	-35.1165	173.2673	1006428	27/01/1958	2/10/2025	6.58	3.10	11.82	1.80	0.20	201.75	68	103.67	105.82	201.75	158.58	8
-1323	Takahue at Crene Road	-35.1837	173.3482	1011596	1/11/2018	2/10/2025	1.00	0.52	1.80	1.80	0.10	32.82	8	15.81	12.83	32.82	30.62	2
1330	Awanui at Slackline	-35.1049	173.2266	1006331	28/02/1972	9/05/1980	7.34	4.13	7.95	1.08	0.50	61.38	9	41.45	34.90	61.38	60.72	1
1335	Tarawhataroa at Puriri Place	-35.1219	173.2684	1006493	31/08/2006	2/10/2025	0.59	0.28	1.28	2.19	0.00	50.30	20	12.52	9.44	50.30	21.70	2
1342	Te Puhi at Meffin Rd	-35.1105	173.3703	1007800	30/03/1990	2/10/2025	1.63	0.90	2.55	1.57	0.00	34.96	36	22.08	22.59	34.96	31.40	3
1351	Victoria at Victoria Valley Road	-35.1517	173.4157	1012697	16/08/2006	2/10/2025	1.03	0.61	1.47	1.42	0.13	27.60	20	12.48	12.40	27.60	20.88	2
1903	Oruru at Saleyards	-35.0791	173.5115	1007524	15/12/1988	2/10/2025	2.47	1.37	3.95	1.60	0.30	64.62	38	34.82	34.73	64.62	50.46	4
1909	Peria at Honeymoon Valley	-35.1207	173.4931	1007924	25/07/1974	9/04/1981	1.23	0.78	2.08	1.69	0.20	27.40	8	18.37	20.50	27.40	26.45	1
2612	Kaeo at Waiare Road	-35.1169	173.7981	1010288	25/07/2008	2/10/2025	2.31	1.01	4.78	2.07	0.10	85.50	18	45.38	43.98	85.50	71.32	4
3432	Rangitane at Stirlings	-35.1928	173.9667	1017068	10/10/2001	2/10/2025	0.75	0.40	1.52	2.01	0.00	39.55	25	14.68	13.26	39.55	23.84	4

Site ID	Station Name	latitude	longitude	NZ Segments	Start Date	End Date	Mean Flow (m^3/s)	Median' Flow (m^3/s)	Sd Flow (m^3/s)	Cv Flow	Min Flow (m^3/s)	Max Flow (m^3/s)	Record Length (years)	Mean Annual Max (m^3/s)	Median Annual Max (m^3/s)	Max Annual Max (m^3/s)	RL 10 (m^3/s)	N Daily Exceed RL10
3436	Waipapa at Doonside Road	-35.2016	173.956	1017107	4/12/2012	2/10/2025	1.12	0.50	2.70	2.42	0.00	55.89	14	24.08	22.87	55.89	47.12	1
3503	Puketotara at Backblocks	-35.2436	173.8878	1016338	10/09/1975	31/01/1989	2.45	0.79	7.95	3.24	0.09	140.16	15	66.44	65.38	140.16	102.12	1
3506	Maungaparerua at Tyrees Ford	-35.2347	173.8843	1016203	22/11/1967	2/10/2025	0.52	0.21	1.38	2.65	0.01	33.99	59	13.30	13.09	33.99	21.21	6
3515	Kerikeri at Peacock Garden	-35.2151	173.9543	1017189	18/12/2012	2/10/2025	4.01	2.02	8.71	2.17	0.20	153.08	14	78.37	73.55	153.08	126.30	3
3518	Waiwhakangaro ngaro at Baxters	-35.2585	173.8946	1016442	22/07/1980	7/09/1988	0.08	0.02	0.21	2.54	0.00	6.74	9	2.06	1.57	6.74	3.95	1
3523	Puketotara at BOI Golf Club	-35.2228	173.9444	1017291	8/12/2011	2/10/2025	1.68	0.93	3.51	2.09	0.10	63.31	15	35.22	31.45	63.31	56.81	4
3707	Waiaruhe at Puketona	-35.3022	173.96	1022868	2/02/1984	2/10/2025	5.05	2.44	9.70	1.92	0.29	189.09	42	75.87	61.13	189.09	133.41	6
3710	Whangai at Wiroa Rd	-35.2729	173.8563	1016579	1/10/1979	15/08/1984	0.11	0.05	0.37	3.23	0.00	5.93	6	2.97	2.47	5.93	8.22	0
3722	Waitangi at Wakelins	-35.2763	174.0475	1022607	22/02/1979	31/10/2025	8.35	4.27	16.08	1.93	0.34	490.01	47	154.22	135.49	490.01	258.26	5
3725	Waitangi at Waimate North Rd	-35.2968	173.9016	1022800	4/10/2011	2/10/2025	1.62	0.81	3.41	2.10	0.03	65.63	15	32.70	32.75	65.63	55.86	4
3806	Kawakawa at SHBr	-35.3761	174.062	1023578	15/12/1961	5/04/1968	6.44	2.70	9.29	1.44	0.10	123.90	8	51.27	39.01	123.90	95.16	1
3817	Tirohanga at Below Old Mill	-35.3795	174.1039	1024784	15/10/2010	2/10/2025	1.64	0.80	3.80	2.31	0.06	74.14	16	34.13	27.82	74.14	60.77	3
3819	Waiharakeke at Willowbank	-35.3944	174.0197	1023766	19/04/1967	2/10/2025	5.72	2.30	10.08	1.76	0.01	190.29	59	72.05	64.41	190.29	120.89	10
45504	Makarau at Coles	-36.5566	174.513	2007568	31/03/1989	31/07/2017	1.19	0.41	4.11	3.44	0.04	104.45	29	52.53	49.11	104.45	84.94	4

Site ID	Station Name	latitude	longitude	NZ Segments	Start Date	End Date	Mean Flow (m^3/s)	Median' Flow (m^3/s)	Sd Flow (m^3/s)	Cv Flow	Min Flow (m^3/s)	Max Flow (m^3/s)	Record Length (years)	Mean Annual Max (m^3/s)	Median Annual Max (m^3/s)	Max Annual Max (m^3/s)	RL 10 (m^3/s)	N Daily Exceed RL10
45702	Waiwhiu at Dome Shadow	-36.3511	174.631	2004653	24/11/1967	31/07/2017	0.30	0.11	0.86	2.82	0.01	20.36	51	9.02	8.40	20.36	14.63	7
45903	Topuni at Old North Rd	-36.2041	174.458	1062521	1/01/1977	22/05/1986	0.02	0.00	0.05	2.86	0.00	0.69	10	0.54	0.59	0.69	0.68	2
46020	Hakaru at Topuni Creek Farm	-36.2036	174.4929	1063284	15/09/2011	2/10/2025	2.15	0.85	5.24	2.43	0.11	107.41	15	49.21	41.34	107.41	79.82	2
46609	Mangere at Kara Weir	-35.7101	174.2372	1040689	24/04/1975	5/08/1993	0.40	0.20	1.13	2.86	0.00	31.81	19	11.17	7.44	31.81	24.63	3
46611	Kaihu at Gorge	-35.7615	173.6864	1043364	5/03/1970	2/10/2025	4.30	2.58	6.65	1.55	0.49	197.32	56	67.63	63.33	197.32	113.19	5
46612	Kaihu at Maropiu	-35.7993	173.7341	1044595	3/10/1958	1/03/1971	6.99	3.50	13.02	1.86	0.60	203.56	14	105.79	89.92	203.56	186.09	4
46618	Mangakahia at Gorge	-35.628	173.8512	1036951	8/12/1960	2/10/2025	10.48	5.38	18.85	1.80	0.71	429.32	66	186.40	186.09	429.32	298.62	7
46625	Hikurangi at Moengawahine	-35.6459	174.0414	1038521	10/04/1960	2/10/2025	5.48	1.96	13.34	2.43	0.10	207.60	66	118.43	120.18	207.60	174.68	4
46626	Mangakahia at Titoki Br	-35.7327	174.0529	1045514	1/03/1983	2/10/2025	25.19	12.90	43.55	1.73	1.40	996.91	43	422.00	417.09	996.91	722.45	5
46627	Waiotu at SHBr	-35.5328	174.2288	1032423	20/10/1987	2/10/2025	4.37	1.65	9.40	2.15	0.10	134.04	39	79.66	82.26	134.04	116.60	4
46632	Whakapara at Cableway	-35.5378	174.2734	1033900	10/12/1959	2/10/2025	6.84	2.90	14.80	2.16	0.16	249.27	67	129.48	133.83	249.27	205.93	10
46639	Wairua at Lewis Bridge	-35.6324	174.199	1039892	2/11/1956	1/01/1971	22.47	11.30	27.30	1.21	0.70	201.80	16	117.94	121.45	201.80	181.09	7
46641	Waipao at Draffins Rd	-35.7262	174.1278	1046842	22/06/1979	2/10/2025	0.70	0.49	0.92	1.32	0.03	21.51	47	8.34	7.88	21.51	13.42	6
46644	Wairua at Purua	-35.6523	174.1512	1040112	21/03/1960	2/10/2025	19.83	8.95	29.73	1.50	0.60	296.66	66	183.75	192.41	296.66	261.10	9
46645	Kokopu at McBeths	-35.7252	174.1904	1046866	29/06/1977	5/08/1986	0.08	0.02	0.21	2.82	0.00	3.26	10	2.09	2.23	3.26	2.88	1
46646	Mangere at KnightsRd	-35.6975	174.1444	1040554	15/02/1983	2/10/2025	1.76	0.70	4.22	2.39	0.00	85.49	43	39.83	41.14	85.49	62.52	5

Site ID	Station Name	latitude	longitude	NZ Segments	Start Date	End Date	Mean Flow (m^3/s)	Median' Flow (m^3/s)	Sd Flow (m^3/s)	Cv Flow	Min Flow (m^3/s)	Max Flow (m^3/s)	Record Length (years)	Mean Annual Max (m^3/s)	Median Annual Max (m^3/s)	Max Annual Max (m^3/s)	RL 10 (m^3/s)	N Daily Exceed RL10
46651	Manganui at Permanent Station	-35.9617	174.1136	1053888	21/05/1960	2/10/2025	8.52	3.00	16.78	1.97	0.10	364.48	66	135.08	141.44	364.48	223.42	10
46660	Puketurua at Puketitoi	-35.6604	174.0693	1038715	3/01/1964	5/08/1986	0.07	0.02	0.22	3.06	0.00	4.55	23	2.28	2.16	4.55	3.30	2
46674	Mangahahuru at County Weir	-35.64	174.312	1041523	15/12/1968	2/10/2025	0.63	0.34	1.29	2.06	0.04	26.03	58	12.01	12.77	26.03	19.87	5
46902	Waipoua at SH12	-35.6528	173.57	1035723	30/05/2007	2/10/2025	2.93	1.51	5.12	1.74	0.27	121.54	19	49.80	42.40	121.54	90.96	2
47527	Opahi at Pond	-35.4061	173.7225	1021073	3/02/1966	24/01/1994	0.32	0.09	0.90	2.82	0.00	36.32	29	8.16	8.33	36.32	14.84	1
47595	Punakitere at Taheke	-35.4638	173.6606	1027462	16/12/1994	2/10/2025	7.20	3.44	12.87	1.79	0.36	160.69	32	109.13	116.68	160.69	150.95	6
47804	Waipapa at Forest Ranger	-35.2738	173.6881	1015214	1/04/1978	29/10/2025	4.82	2.23	10.37	2.15	0.25	300.40	48	101.00	95.03	300.40	166.43	8
48015	Mangamuka at Gorge	-35.1991	173.5002	1013115	31/03/1976	20/01/1994	1.14	0.60	1.89	1.67	0.10	28.36	19	15.98	16.21	28.36	24.40	2
4901	Ngunguru at Dugmores Rock	-35.5988	174.4324	1041091	22/08/1969	2/10/2025	0.48	0.22	1.36	2.85	0.03	37.79	57	14.59	13.21	37.79	25.35	7
4914	Ngunguru at Coal Hill Lane Br	-35.6434	174.4115	1041554	29/08/2019	2/10/2025	1.90	0.90	4.74	2.49	0.20	100.11	7	51.36	41.03	100.11	97.12	2
5513	Glenbervie at Quarry	-35.6461	174.3472	1041582	1/01/1977	5/01/1987	0.02	0.01	0.07	3.15	0.00	1.91	11	0.70	0.54	1.91	1.31	1
5519	Waiarohia at Russell Rd	-35.7117	174.3149	1042267	31/08/1957	3/01/1968	0.71	0.30	1.88	2.63	0.00	45.32	12	15.99	14.33	45.32	30.52	1
5527	Waiarohia at Lovers Lane	-35.7242	174.3168	1048290	17/10/1979	2/10/2025	0.40	0.16	1.21	3.01	0.02	39.03	47	11.72	8.37	39.03	23.98	5
5528	Raumanga at Bernard St	-35.7331	174.3136	1048393	31/10/1979	2/10/2025	0.39	0.21	0.88	2.25	0.03	27.23	47	8.62	7.42	27.23	15.58	5

Site ID	Station Name	latitude	longitude	NZ Segments	Start Date	End Date	Mean Flow (m^3/s)	Median' Flow (m^3/s)	Sd Flow (m^3/s)	Cv Flow	Min Flow (m^3/s)	Max Flow (m^3/s)	Record Length (years)	Mean Annual Max (m^3/s)	Median Annual Max (m^3/s)	Max Annual Max (m^3/s)	RL 10 (m^3/s)	N Daily Exceed RL10
5538	Hatea at Whareora Rd	-35.702	174.3307	1042220	30/06/1986	2/10/2025	1.21	0.58	3.50	2.90	0.04	121.60	40	36.63	25.83	121.60	80.73	3
5659	Otaika at Kay	-35.7782	174.2782	1048742	27/01/2011	2/10/2025	0.86	0.44	1.79	2.08	0.04	43.33	15	18.65	18.80	43.33	33.78	1
5901	Ruakaka at Flyger Rd	-35.8683	174.4037	1054472	19/03/1984	2/10/2025	0.85	0.27	2.56	3.01	0.00	70.00	42	27.16	24.63	70.00	45.03	4
5911	Waiwarawara at Wilsons Dam	-35.8973	174.4165	1054779	23/10/1991	13/07/1998	0.07	0.03	0.23	3.22	0.00	4.97	8	2.28	1.30	4.97	4.97	0
6004	Ahuroa at Rowntrees	-35.9928	174.4111	1055789	28/02/1969	7/01/1976	2.07	0.90	5.89	2.85	0.10	99.66	8	54.39	54.25	99.66	89.53	1
6007	Waionehu at McLean Rd	-36.0085	174.4587	1056117	12/05/1983	18/06/2015	0.52	0.20	1.31	2.52	0.00	21.29	33	12.20	12.41	21.29	17.93	6
6015	North at Applecross Rd	-35.9379	174.4107	1055206	22/12/1982	2/10/2025	0.98	0.42	2.20	2.24	0.00	46.48	44	20.45	19.98	46.48	34.63	6
6016	Waihoihoi at St Marys Rd	-36.0053	174.4298	1055911	31/01/1984	2/10/2025	0.58	0.30	1.13	1.94	0.00	25.40	42	11.01	11.15	25.40	16.76	5
6018	Ahuroa at Braigh	-36.001	174.412	1055884	30/08/1983	2/10/2025	1.36	0.60	3.03	2.23	0.00	57.17	43	30.27	30.92	57.17	45.06	7
802	Selwyn Swamp at Big Flat Rd	-34.9192	173.1701	1003880	25/08/1965	2/10/2025	0.04	0.02	0.06	1.65	0.00	1.40	61	0.55	0.48	1.40	0.97	7

Appendix B Spatial coverage of daily events exceeding 10-year threshold

Date	n_sites	Total of Number Available Sites	% Coverage (proportion)	Month	Season	Sites ID
13/02/2023	15	45	0.33	2	Summer	1046651; 46611; 46632; 46641; 46646; 46674; 4914; 5527; 5528; 5538; 5659; 5901; 6015; 6016; 6018
18/08/2022	12	45	0.27	8	Winter	1316; 1323; 1335; 1342; 1351; 1903; 2612; 3432; 3515; 3523; 3725; 47804
29/01/2011	11	41	0.27	1	Summer	3722; 3819; 46626; 46627; 46632; 46646; 47595; 4901; 5901; 6016; 6018
14/02/2023	11	45	0.24	2	Summer	1046651; 46020; 46618; 46626; 46641; 46644; 46651; 47595; 6015; 6016; 6018
10/07/2007	10	38	0.26	7	Winter	1046651; 1335; 1903; 3432; 3506; 46611; 46618; 46902; 47804; 5528
18/07/2020	10	45	0.22	7	Winter	1316; 3707; 3722; 3819; 46632; 46644; 47595; 4914; 5901; 6015
29/03/2007	9	37	0.24	3	Autumn	3432; 3506; 3722; 46627; 47804; 4901; 5527; 5528; 6016
19/03/2012	6	44	0.14	3	Autumn	2612; 3523; 46674; 4901; 5527; 5538
25/07/2022	6	45	0.13	7	Winter	2612; 3432; 3515; 3523; 3707; 3725
10/07/2014	5	46	0.11	7	Winter	3817; 3819; 46646; 47595; 5527
17/02/1966	4	13	0.31	2	Summer	46618; 46625; 47527; 5519
8/03/1988	4	34	0.12	3	Autumn	46626; 46627; 46644; 46646
20/06/2002	4	35	0.11	6	Winter	45702; 46625; 6007; 6015
10/06/2014	4	46	0.09	6	Winter	3817; 46618; 46902; 5528

Date	n_sites	Total of Number Available Sites	% Coverage (proportion)	Month	Season	Sites ID
4/04/1968	3	15	0.2	4	Autumn	3806; 3819; 46639
15/02/1969	3	15	0.2	2	Summer	45702; 46632; 46674
14/06/1975	3	20	0.15	6	Winter	3506; 45702; 4901
20/07/1977	3	24	0.13	7	Winter	46609; 4901; 5513
7/03/1988	3	34	0.09	3	Autumn	1046651; 46611; 5538
6/01/1989	3	34	0.09	1	Summer	46632; 46674; 6015
2/06/1997	3	35	0.09	6	Winter	3707; 46627; 6007
26/07/1998	3	34	0.09	7	Winter	6007; 6016; 6018
2/12/2001	3	35	0.09	12	Summer	1046651; 46618; 47804
21/06/2002	3	35	0.09	6	Winter	1316; 3819; 46626
28/03/2003	3	35	0.09	3	Autumn	1316; 1903; 46625
12/07/2014	3	46	0.07	7	Winter	3707; 3819; 47595
31/08/2014	3	46	0.07	8	Winter	2612; 3436; 3515
21/06/2018	3	43	0.07	6	Winter	46632; 46641; 46646
17/07/2020	3	45	0.07	7	Winter	3506; 3523; 3725
11/03/1971	2	16	0.13	3	Autumn	3506; 46674
17/07/1973	2	18	0.11	7	Winter	46632; 6004
13/01/1976	2	20	0.1	1	Summer	1909; 45702
14/01/1976	2	20	0.1	1	Summer	46632; 46651
22/06/1980	2	28	0.07	6	Winter	46611; 46641
20/03/1981	2	29	0.07	3	Autumn	3518; 3722
25/01/1986	2	36	0.06	1	Summer	1046651; 48015
10/03/1988	2	34	0.06	3	Autumn	46625; 48015
30/03/1995	2	35	0.06	3	Autumn	46644; 5901
30/12/1996	2	35	0.06	12	Summer	45702; 6015
25/07/1998	2	34	0.06	7	Winter	45504; 6007

Date	n_sites	Total of Number Available Sites	% Coverage (proportion)	Month	Season	Sites ID
6/08/2006	2	35	0.06	8	Winter	6007; 6018
7/02/2007	2	37	0.05	2	Summer	1903; 47804
11/07/2007	2	38	0.05	7	Winter	46626; 46651
9/07/2014	2	46	0.04	7	Winter	3707; 3817
11/07/2014	2	46	0.04	7	Winter	3819; 47595
19/08/2022	2	45	0.04	8	Winter	1314; 1316
11/11/2022	2	45	0.04	11	Spring	46641; 5527
9/05/2023	2	45	0.04	5	Autumn	1351; 3725
24/02/1958	1	3	0.33	2	Summer	1316
26/06/1960	1	8	0.13	6	Winter	46651
1/07/1960	1	8	0.13	7	Winter	46651
2/07/1960	1	8	0.13	7	Winter	46651
3/07/1960	1	8	0.13	7	Winter	46651
4/07/1960	1	8	0.13	7	Winter	46651
8/06/1961	1	9	0.11	6	Winter	46612
9/06/1961	1	9	0.11	6	Winter	46612
31/05/1962	1	10	0.1	5	Autumn	46618
2/02/1967	1	13	0.08	2	Summer	46660
3/02/1967	1	13	0.08	2	Summer	46618
17/11/1967	1	14	0.07	11	Spring	46612
5/04/1968	1	15	0.07	4	Autumn	46639
6/04/1968	1	14	0.07	4	Autumn	46639
11/04/1968	1	14	0.07	4	Autumn	46639
12/04/1968	1	14	0.07	4	Autumn	46639
16/02/1969	1	15	0.07	2	Summer	46639
17/02/1969	1	15	0.07	2	Summer	46639

Date	n_sites	Total of Number Available Sites	% Coverage (proportion)	Month	Season	Sites ID
21/05/1969	1	16	0.06	5	Autumn	46612
15/06/1969	1	16	0.06	6	Winter	802
3/11/1970	1	18	0.06	11	Spring	46660
4/08/1971	1	16	0.06	8	Winter	3819
5/08/1971	1	16	0.06	8	Winter	3819
8/03/1972	1	18	0.06	3	Autumn	45702
10/10/1972	1	18	0.06	10	Spring	46611
20/11/1972	1	18	0.06	11	Spring	802
23/02/1974	1	18	0.06	2	Summer	3506
30/05/1975	1	20	0.05	5	Autumn	45702
15/01/1976	1	20	0.05	1	Summer	46651
9/08/1976	1	21	0.05	8	Winter	46609
6/09/1976	1	21	0.05	9	Spring	46632
7/09/1976	1	21	0.05	9	Spring	46632
18/06/1978	1	25	0.04	6	Winter	46644
13/06/1979	1	26	0.04	6	Winter	3722
31/07/1979	1	27	0.04	7	Winter	3503
23/01/1980	1	30	0.03	1	Summer	1330
14/02/1980	1	30	0.03	2	Summer	47804
15/03/1980	1	30	0.03	3	Autumn	45903
8/06/1983	1	32	0.03	6	Winter	46645
15/08/1984	1	36	0.03	8	Winter	45903
15/12/1984	1	36	0.03	12	Summer	1046651
16/02/1985	1	36	0.03	2	Summer	1046651
9/03/1988	1	34	0.03	3	Autumn	46644
11/03/1988	1	34	0.03	3	Autumn	3819

Date	n_sites	Total of Number Available Sites	% Coverage (proportion)	Month	Season	Sites ID
7/01/1989	1	34	0.03	1	Summer	46644
8/01/1989	1	34	0.03	1	Summer	46644
4/08/1989	1	34	0.03	8	Winter	3707
8/09/1989	1	34	0.03	9	Spring	46644
26/11/1989	1	34	0.03	11	Spring	46609
29/03/1995	1	35	0.03	3	Autumn	45504
23/06/1996	1	35	0.03	6	Winter	45504
30/06/1997	1	35	0.03	6	Winter	6018
9/09/1997	1	35	0.03	9	Spring	47804
27/08/1998	1	34	0.03	8	Winter	1316
26/04/1999	1	34	0.03	4	Autumn	802
28/06/2000	1	34	0.03	6	Winter	802
29/06/2000	1	34	0.03	6	Winter	4901
11/12/2000	1	34	0.03	12	Summer	4901
1/09/2001	1	34	0.03	9	Spring	45504
2/05/2003	1	35	0.03	5	Autumn	802
29/02/2004	1	35	0.03	2	Summer	1316
6/07/2005	1	35	0.03	7	Winter	6018
16/07/2007	1	38	0.03	7	Winter	6007
23/02/2008	1	38	0.03	2	Summer	47804
15/12/2011	1	44	0.02	12	Summer	1342
24/10/2021	1	45	0.02	10	Spring	1342
21/03/2022	1	45	0.02	3	Autumn	46641
10/01/2023	1	45	0.02	1	Summer	5528
15/02/2023	1	45	0.02	2	Summer	46651
24/02/2023	1	45	0.02	2	Summer	46020

Date	n_sites	Total of Number Available Sites	% Coverage (proportion)	Month	Season	Sites ID
4/05/2023	1	45	0.02	5	Autumn	802
5/05/2023	1	45	0.02	5	Autumn	802
4/04/2025	1	45	0.02	4	Autumn	1323

Appendix C Identified Events with ENSO and SAM index

Date	n_sites	Total of Number Available Sites	% Coverage	Month	Season	ENSO index	SAM index	ENSO phase	SAM phase	AR flag	Cyclone Present	Storm type	Flood Spatial extend
13/02/2023	15	45	0.33	2	Summer	-0.46	0.45	Neutral	Neutral	TRUE	TRUE	ETC_AR	Wide spread
18/08/2022	12	45	0.27	8	Winter	-0.97	0.66	LaNina	Neutral	FALSE	FALSE	Convective	Wide spread
29/01/2011	11	41	0.27	1	Summer	-1.54	0.48	LaNina	Neutral	FALSE	TRUE	ETC	Wide spread
14/02/2023	11	45	0.24	2	Summer	-0.46	0.45	Neutral	Neutral	TRUE	TRUE	ETC_AR	Wide spread
10/07/2007	10	38	0.26	7	Winter	-0.59	-2.67	LaNina	Negative	TRUE	TRUE	ETC_AR	Wide spread
18/07/2020	10	45	0.22	7	Winter	-0.3	-0.97	Neutral	Negative	TRUE	TRUE	ETC_AR	Wide spread
29/03/2007	9	37	0.24	3	Autumn	-0.18	-0.77	Neutral	Negative	TRUE	TRUE	ETC_AR	Wide spread
19/03/2012	6	44	0.14	3	Autumn	-0.61	0.48	LaNina	Neutral	FALSE	FALSE	Convective	moderate spread
25/07/2022	6	45	0.13	7	Winter	-0.69	1.24	LaNina	Positive	FALSE	FALSE	Convective	moderate spread
10/07/2014	5	46	0.11	7	Winter	-0.06	0.68	Neutral	Neutral	FALSE	FALSE	Convective	moderate spread
17/02/1966	4	13	0.31	2	Summer	0.8	-2.94	ElNino	Negative	FALSE	FALSE	Convective	moderate spread
8/03/1988	4	34	0.12	3	Autumn	0.1	-2.01	Neutral	Negative	FALSE	FALSE	Convective	moderate spread
20/06/2002	4	35	0.11	6	Winter	0.72	-0.43	ElNino	Neutral	FALSE	FALSE	Convective	moderate spread
10/06/2014	4	46	0.09	6	Winter	0.23	-0.21	Neutral	Neutral	FALSE	FALSE	Convective	moderate spread
4/04/1968	3	15	0.2	4	Autumn	-0.72	-2.72	LaNina	Negative	FALSE	FALSE	Convective	localised
15/02/1969	3	15	0.2	2	Summer	1.11	-3.14	ElNino	Negative	FALSE	FALSE	Convective	localised
14/06/1975	3	20	0.15	6	Winter	-1.5	-0.35	LaNina	Neutral	FALSE	FALSE	Convective	localised
20/07/1977	3	24	0.13	7	Winter	0.09	-1.82	Neutral	Negative	FALSE	FALSE	Convective	localised
7/03/1988	3	34	0.09	3	Autumn	0.1	-2.01	Neutral	Negative	FALSE	FALSE	Convective	localised
6/01/1989	3	34	0.09	1	Summer	-1.97	-0.02	LaNina	Neutral	FALSE	FALSE	Convective	localised
2/06/1997	3	35	0.09	6	Winter	1.09	0.69	ElNino	Neutral	FALSE	FALSE	Convective	localised
26/07/1998	3	34	0.09	7	Winter	-0.99	2.13	LaNina	Positive	FALSE	FALSE	Convective	localised
2/12/2001	3	35	0.09	12	Summer	-0.41	1.16	Neutral	Positive	FALSE	FALSE	Convective	localised

Date	n_sites	Total of Number Available Sites	% Coverage	Month	Season	ENSO index	SAM index	ENSO phase	SAM phase	AR flag	Cyclone Present	Storm type	Flood Spatial extend
21/06/2002	3	35	0.09	6	Winter	0.72	-0.43	ElNino	Neutral	FALSE	FALSE	Convective	localised
28/03/2003	3	35	0.09	3	Autumn	0.36	-0.07	Neutral	Neutral	FALSE	FALSE	Convective	localised
12/07/2014	3	46	0.07	7	Winter	-0.06	0.68	Neutral	Neutral	FALSE	FALSE	Convective	localised
31/08/2014	3	46	0.07	8	Winter	-0.03	1.97	Neutral	Positive	FALSE	FALSE	Convective	localised
21/06/2018	3	43	0.07	6	Winter	0.04	-1.57	Neutral	Negative	FALSE	FALSE	Convective	localised
17/07/2020	3	45	0.07	7	Winter	-0.3	-0.97	Neutral	Negative	TRUE	TRUE	ETC_AR	localised
11/03/1971	2	16	0.13	3	Autumn	-1.36	2.02	LaNina	Positive	FALSE	FALSE	Convective	localised
17/07/1973	2	18	0.11	7	Winter	-1.54	2.57	LaNina	Positive	FALSE	FALSE	Convective	localised
13/01/1976	2	20	0.1	1	Summer	-2.01	-1.17	LaNina	Negative	FALSE	FALSE	Convective	localised
14/01/1976	2	20	0.1	1	Summer	-2.01	-1.17	LaNina	Negative	FALSE	FALSE	Convective	localised
22/06/1980	2	28	0.07	6	Winter	0.21	3.19	Neutral	Positive	FALSE	FALSE	Convective	localised
20/03/1981	2	29	0.07	3	Autumn	-0.64	-2.47	LaNina	Negative	FALSE	FALSE	Convective	localised
25/01/1986	2	36	0.06	1	Summer	-0.66	0.37	LaNina	Neutral	FALSE	FALSE	Convective	localised
10/03/1988	2	34	0.06	3	Autumn	0.1	-2.01	Neutral	Negative	FALSE	FALSE	Convective	localised
30/03/1995	2	35	0.06	3	Autumn	0.46	-1.12	Neutral	Negative	FALSE	FALSE	Convective	localised
30/12/1996	2	35	0.06	12	Summer	-0.64	0.03	LaNina	Neutral	FALSE	FALSE	Convective	localised
25/07/1998	2	34	0.06	7	Winter	-0.99	2.13	LaNina	Positive	FALSE	FALSE	Convective	localised
6/08/2006	2	35	0.06	8	Winter	0.31	-2.64	Neutral	Negative	FALSE	FALSE	Convective	localised
7/02/2007	2	37	0.05	2	Summer	0.13	2.36	Neutral	Positive	FALSE	FALSE	Convective	localised
11/07/2007	2	38	0.05	7	Winter	-0.59	-2.67	LaNina	Negative	TRUE	TRUE	ETC_AR	localised
9/07/2014	2	46	0.04	7	Winter	-0.06	0.68	Neutral	Neutral	FALSE	FALSE	Convective	localised
11/07/2014	2	46	0.04	7	Winter	-0.06	0.68	Neutral	Neutral	FALSE	FALSE	Convective	localised
19/08/2022	2	45	0.04	8	Winter	-0.97	0.66	LaNina	Neutral	FALSE	FALSE	Convective	localised
11/11/2022	2	45	0.04	11	Spring	-0.9	3.71	LaNina	Positive	FALSE	FALSE	Convective	localised
9/05/2023	2	45	0.04	5	Autumn	0.46	1.8	Neutral	Positive	FALSE	FALSE	Convective	localised
24/02/1958	1	3	0.33	2	Summer	1.49	-2.84	ElNino	Negative	FALSE	FALSE	Convective	localised

Date	n_sites	Total of Number Available Sites	% Coverage	Month	Season	ENSO index	SAM index	ENSO phase	SAM phase	AR flag	Cyclone Present	Storm type	Flood Spatial extend
26/06/1960	1	8	0.13	6	Winter	-0.49	-0.17	Neutral	Neutral	FALSE	FALSE	Convective	localised
1/07/1960	1	8	0.13	7	Winter	-0.41	0.31	Neutral	Neutral	FALSE	FALSE	Convective	localised
2/07/1960	1	8	0.13	7	Winter	-0.41	0.31	Neutral	Neutral	FALSE	FALSE	Convective	localised
3/07/1960	1	8	0.13	7	Winter	-0.41	0.31	Neutral	Neutral	FALSE	FALSE	Convective	localised
4/07/1960	1	8	0.13	7	Winter	-0.41	0.31	Neutral	Neutral	FALSE	FALSE	Convective	localised
8/06/1961	1	9	0.11	6	Winter	-0.06	-0.4	Neutral	Neutral	FALSE	FALSE	Convective	localised
9/06/1961	1	9	0.11	6	Winter	-0.06	-0.4	Neutral	Neutral	FALSE	FALSE	Convective	localised
31/05/1962	1	10	0.1	5	Autumn	-0.89	-0.66	LaNina	Neutral	FALSE	FALSE	Convective	localised
2/02/1967	1	13	0.08	2	Summer	-0.64	-4.22	LaNina	Negative	FALSE	FALSE	Convective	localised
3/02/1967	1	13	0.08	2	Summer	-0.64	-4.22	LaNina	Negative	FALSE	FALSE	Convective	localised
17/11/1967	1	14	0.07	11	Spring	-0.62	-2.17	LaNina	Negative	FALSE	FALSE	Convective	localised
5/04/1968	1	15	0.07	4	Autumn	-0.72	-2.72	LaNina	Negative	FALSE	FALSE	Convective	localised
6/04/1968	1	14	0.07	4	Autumn	-0.72	-2.72	LaNina	Negative	FALSE	FALSE	Convective	localised
11/04/1968	1	14	0.07	4	Autumn	-0.72	-2.72	LaNina	Negative	FALSE	FALSE	Convective	localised
12/04/1968	1	14	0.07	4	Autumn	-0.72	-2.72	LaNina	Negative	FALSE	FALSE	Convective	localised
16/02/1969	1	15	0.07	2	Summer	1.11	-3.14	ElNino	Negative	FALSE	FALSE	Convective	localised
17/02/1969	1	15	0.07	2	Summer	1.11	-3.14	ElNino	Negative	FALSE	FALSE	Convective	localised
21/05/1969	1	16	0.06	5	Autumn	0.35	1.39	Neutral	Positive	FALSE	FALSE	Convective	localised
15/06/1969	1	16	0.06	6	Winter	-0.04	-0.88	Neutral	Negative	FALSE	FALSE	Convective	localised
3/11/1970	1	18	0.06	11	Spring	-1.13	0.45	LaNina	Neutral	FALSE	FALSE	Convective	localised
4/08/1971	1	16	0.06	8	Winter	-1.1	-0.78	LaNina	Negative	FALSE	FALSE	Convective	localised
5/08/1971	1	16	0.06	8	Winter	-1.1	-0.78	LaNina	Negative	FALSE	FALSE	Convective	localised
8/03/1972	1	18	0.06	3	Autumn	-0.19	-2.05	Neutral	Negative	FALSE	FALSE	Convective	localised
10/10/1972	1	18	0.06	10	Spring	1.54	-1.48	ElNino	Negative	FALSE	FALSE	Convective	localised
20/11/1972	1	18	0.06	11	Spring	1.9	1.39	ElNino	Positive	FALSE	FALSE	Convective	localised
23/02/1974	1	18	0.06	2	Summer	-1.66	1.82	LaNina	Positive	FALSE	FALSE	Convective	localised

Date	n_sites	Total of Number Available Sites	% Coverage	Month	Season	ENSO index	SAM index	ENSO phase	SAM phase	AR flag	Cyclone Present	Storm type	Flood Spatial extend
30/05/1975	1	20	0.05	5	Autumn	-1.13	-3.33	LaNina	Negative	FALSE	FALSE	Convective	localised
15/01/1976	1	20	0.05	1	Summer	-2.01	-1.17	LaNina	Negative	FALSE	FALSE	Convective	localised
9/08/1976	1	21	0.05	8	Winter	0.12	0.3	Neutral	Neutral	FALSE	FALSE	Convective	localised
6/09/1976	1	21	0.05	9	Spring	0.3	1.67	Neutral	Positive	FALSE	FALSE	Convective	localised
7/09/1976	1	21	0.05	9	Spring	0.3	1.67	Neutral	Positive	FALSE	FALSE	Convective	localised
18/06/1978	1	25	0.04	6	Winter	-0.71	0.83	LaNina	Positive	FALSE	FALSE	Convective	localised
13/06/1979	1	26	0.04	6	Winter	-0.29	2.52	Neutral	Positive	FALSE	FALSE	Convective	localised
31/07/1979	1	27	0.04	7	Winter	-0.47	3.14	Neutral	Positive	FALSE	FALSE	Convective	localised
23/01/1980	1	30	0.03	1	Summer	0.54	0.01	ElNino	Neutral	FALSE	FALSE	Convective	localised
14/02/1980	1	30	0.03	2	Summer	0.22	-1.75	Neutral	Negative	FALSE	FALSE	Convective	localised
15/03/1980	1	30	0.03	3	Autumn	0.03	-2.58	Neutral	Negative	FALSE	FALSE	Convective	localised
8/06/1983	1	32	0.03	6	Winter	0.54	0.38	ElNino	Neutral	FALSE	FALSE	Convective	localised
15/08/1984	1	36	0.03	8	Winter	-0.24	-2.33	Neutral	Negative	FALSE	FALSE	Convective	localised
15/12/1984	1	36	0.03	12	Summer	-1.34	-3.22	LaNina	Negative	FALSE	FALSE	Convective	localised
16/02/1985	1	36	0.03	2	Summer	-0.72	-0.02	LaNina	Neutral	FALSE	FALSE	Convective	localised
9/03/1988	1	34	0.03	3	Autumn	0.1	-2.01	Neutral	Negative	FALSE	FALSE	Convective	localised
11/03/1988	1	34	0.03	3	Autumn	0.1	-2.01	Neutral	Negative	FALSE	FALSE	Convective	localised
7/01/1989	1	34	0.03	1	Summer	-1.97	-0.02	LaNina	Neutral	FALSE	FALSE	Convective	localised
8/01/1989	1	34	0.03	1	Summer	-1.97	-0.02	LaNina	Neutral	FALSE	FALSE	Convective	localised
4/08/1989	1	34	0.03	8	Winter	-0.53	-1.21	LaNina	Negative	FALSE	FALSE	Convective	localised
8/09/1989	1	34	0.03	9	Spring	-0.3	-0.23	Neutral	Neutral	FALSE	FALSE	Convective	localised
26/11/1989	1	34	0.03	11	Spring	-0.45	0.69	Neutral	Neutral	FALSE	FALSE	Convective	localised
29/03/1995	1	35	0.03	3	Autumn	0.46	-1.12	Neutral	Negative	FALSE	FALSE	Convective	localised
23/06/1996	1	35	0.03	6	Winter	-0.44	-1.4	Neutral	Negative	FALSE	FALSE	Convective	localised
30/06/1997	1	35	0.03	6	Winter	1.09	0.69	ElNino	Neutral	FALSE	FALSE	Convective	localised
9/09/1997	1	35	0.03	9	Spring	2.13	0.69	ElNino	Neutral	FALSE	FALSE	Convective	localised

Date	n_sites	Total of Number Available Sites	% Coverage	Month	Season	ENSO index	SAM index	ENSO phase	SAM phase	AR flag	Cyclone Present	Storm type	Flood Spatial extend
27/08/1998	1	34	0.03	8	Winter	-1.28	2.66	LaNina	Positive	FALSE	FALSE	Convective	localised
26/04/1999	1	34	0.03	4	Autumn	-1.11	2.44	LaNina	Positive	FALSE	FALSE	Convective	localised
28/06/2000	1	34	0.03	6	Winter	-0.79	-0.31	LaNina	Neutral	FALSE	FALSE	Convective	localised
29/06/2000	1	34	0.03	6	Winter	-0.79	-0.31	LaNina	Neutral	FALSE	FALSE	Convective	localised
11/12/2000	1	34	0.03	12	Summer	-0.92	-2.05	LaNina	Negative	FALSE	FALSE	Convective	localised
1/09/2001	1	34	0.03	9	Spring	-0.2	1.46	Neutral	Positive	FALSE	FALSE	Convective	localised
2/05/2003	1	35	0.03	5	Autumn	-0.61	1.04	LaNina	Positive	FALSE	FALSE	Convective	localised
29/02/2004	1	35	0.03	2	Summer	0.23	-3.33	Neutral	Negative	FALSE	FALSE	Convective	localised
6/07/2005	1	35	0.03	7	Winter	-0.23	-0.5	Neutral	Neutral	FALSE	FALSE	Convective	localised
16/07/2007	1	38	0.03	7	Winter	-0.59	-2.67	LaNina	Negative	FALSE	FALSE	Convective	localised
23/02/2008	1	38	0.03	2	Summer	-1.67	1.09	LaNina	Positive	FALSE	FALSE	Convective	localised
15/12/2011	1	44	0.02	12	Summer	-1.06	3.43	LaNina	Positive	FALSE	FALSE	Convective	localised
24/10/2021	1	45	0.02	10	Spring	-0.94	0.8	LaNina	Positive	FALSE	FALSE	Convective	localised
21/03/2022	1	45	0.02	3	Autumn	-0.97	1.28	LaNina	Positive	FALSE	FALSE	Convective	localised
10/01/2023	1	45	0.02	1	Summer	-0.72	4.56	LaNina	Positive	FALSE	FALSE	Convective	localised
15/02/2023	1	45	0.02	2	Summer	-0.46	0.45	Neutral	Neutral	FALSE	FALSE	Convective	localised
24/02/2023	1	45	0.02	2	Summer	-0.46	0.45	Neutral	Neutral	FALSE	FALSE	Convective	localised
4/05/2023	1	45	0.02	5	Autumn	0.46	1.8	Neutral	Positive	FALSE	FALSE	Convective	localised
5/05/2023	1	45	0.02	5	Autumn	0.46	1.8	Neutral	Positive	FALSE	FALSE	Convective	localised
4/04/2025	1	45	0.02	4	Autumn	-0.14	2.68	Neutral	Positive	FALSE	FALSE	Convective	localised

Appendix D Site and frequency of events

Station Id	NZ Segment	Station Name	Number Of Events	Type	Event Dates
3819	1023766	Waiharakeke at Willowbank	10	2	1968-04-04, 1971-08-04, 1971-08-05, 1988-03-11, 2002-06-21, 2011-01-29, 2014-07-10, 2014-07-11, 2014-07-12, 2020-07-18
46632	1033900	Whakapara at Cableway	10	2	1969-02-15, 1973-07-17, 1976-01-14, 1976-09-06, 1976-09-07, 1989-01-06, 2011-01-29, 2018-06-21, 2020-07-18, 2023-02-13
46651	1053888	Manganui at Permanent Station	10	3	1960-06-26, 1960-07-01, 1960-07-02, 1960-07-03, 1960-07-04, 1976-01-14, 1976-01-15, 2007-07-11, 2023-02-14, 2023-02-15
46644	1040112	Wairua at Purua	9	2	1978-06-18, 1988-03-08, 1988-03-09, 1989-01-07, 1989-01-08, 1989-09-08, 1995-03-30, 2020-07-18, 2023-02-14
1316	1006428	Awanui at School Cut	8	3	1958-02-24, 1998-08-27, 2002-06-21, 2003-03-28, 2004-02-29, 2020-07-18, 2022-08-18, 2022-08-19
47804	1015214	Waipapa at Forest Ranger	8	2	1980-02-14, 1997-09-09, 2001-12-02, 2007-02-07, 2007-03-29, 2007-07-10, 2008-02-23, 2022-08-18
1046651	1037586	Opouteke at Suspension Br	8	2	1984-12-15, 1985-02-16, 1986-01-25, 1988-03-07, 2001-12-02, 2007-07-10, 2023-02-13, 2023-02-14
802	1003880	Selwyn Swamp at Big Flat Rd	7	3	1969-06-15, 1972-11-20, 1999-04-26, 2000-06-28, 2003-05-02, 2023-05-04, 2023-05-05
4901	1041091	Ngunguru at Dugmores Rock	7	3	1975-06-14, 1977-07-20, 2000-06-29, 2000-12-11, 2007-03-29, 2011-01-29, 2012-03-19
6018	1055884	Ahuroa at Braigh	7	1	1997-06-30, 1998-07-26, 2005-07-06, 2006-08-06, 2011-01-29, 2023-02-13, 2023-02-14
46618	1036951	Mangakahia at Gorge	7	3	1962-05-31, 1966-02-17, 1967-02-03, 2001-12-02, 2007-07-10, 2014-06-10,2023-02-14
46639	1039892	Wairua at Lewis Bridge	7	2	1968-04-04, 1968-04-05, 1968-04-06, 1968-04-11, 1968-04-12, 1969-02-16, 1969-02-17
3506	1016203	Maungaparerua at Tyrees Ford	6	2	1971-03-11, 1974-02-23, 1975-06-14, 2007-03-29, 2007-07-10, 2020-07-17

Station Id	NZ Segment	Station Name	Number Of Events	Type	Event Dates
3707	1022868	Waiaruhe at Puketona	6	3	1989-08-04, 1997-06-02, 2014-07-09, 2014-07-12, 2020-07-18, 2022-07-25
6007	1056117	Waionehu at McLean Rd	6	2	1997-06-02, 1998-07-25, 1998-07-26, 2002-06-20, 2006-08-06, 2007-07-16
6015	1055206	North at Applecross Rd	6	1	1989-01-06, 1996-12-30, 2002-06-20, 2020-07-18, 2023-02-13, 2023-02-14
46641	1046842	Waipao at Draffins Rd	6	1	1980-06-22, 2018-06-21, 2022-03-21, 2022-11-11, 2023-02-13, 2023-02-14
47595	1027462	Punakitere at Taheke	6	1	2011-01-29, 2014-07-10, 2014-07-11, 2014-07-12, 2020-07-18, 2023-02-14
3722	1022607	Waitangi at Wakelins	5	2	1979-06-13, 1981-03-20, 2007-03-29, 2011-01-29, 2020-07-18
5527	1048290	Waiarohia at Lovers Lane	5	1	2007-03-29, 2012-03-19, 2014-07-10, 2022-11-11, 2023-02-13
5528	1048393	Raumanga at Bernard St	5	3	2007-03-29, 2007-07-10, 2014-06-10, 2023-01-10, 2023-02-13
6016	1055911	Waihoihoi at St Marys Rd	5	1	1998-07-26, 2007-03-29, 2011-01-29, 2023-02-13, 2023-02-14
46611	1043364	Kaihu at Gorge	5	3	1972-10-10, 1980-06-22, 1988-03-07, 2007-07-10, 2023-02-13
46626	1045514	Mangakahia at Titoki Br	5	3	1988-03-08, 2002-06-21, 2007-07-11, 2011-01-29, 2023-02-14
46646	1040554	Mangere at Knights Rd	5	1	1988-03-08, 2011-01-29, 2014-07-10, 2018-06-21, 2023-02-13
46674	1041523	Mangahahuru at County Weir	5	1	1969-02-15, 1971-03-11, 1989-01-06, 2012-03-19, 2023-02-13
1903	1007524	Oruru at Saleyards	4	2	2003-03-28, 2007-02-07, 2007-07-10, 2022-08-18
2612	1010288	Kaeo at Waiare Road	4	3	2012-03-19, 2014-08-31, 2022-07-25, 2022-08-18
3432	1017068	Rangitane at Stirlings	4	2	2007-03-29, 2007-07-10, 2022-07-25, 2022-08-18
3523	1017291	Puketotara at BOI Golf Club	4	2	2012-03-19, 2020-07-17, 2022-07-25, 2022-08-18
3725	1022800	Waitangi at Waimate North Rd	4	2	2020-07-17, 2022-07-25, 2022-08-18, 2023-05-09
5901	1054472	Ruakaka at Flyger Rd	4	3	1995-03-30, 2011-01-29, 2020-07-18, 2023-02-13
46612	1044595	Kaihu at Maropiu	4	2	1961-06-08, 1961-06-09, 1967-11-17, 1969-05-21
46625	1038521	Hikurangi at Moengawahine	4	2	1966-02-17, 1988-03-10, 2002-06-20, 2003-03-28
46627	1032423	Waiotu at SHBr	4	3	1988-03-08, 1997-06-02, 2007-03-29, 2011-01-29
1342	1007800	Te Puhi at Meffin Rd	3	1	2011-12-15, 2021-10-24, 2022-08-18
3515	1017189	Kerikeri at Peacock Garden	3	2	2014-08-31, 2022-07-25, 2022-08-18
3817	1024784	Tirohanga at Below Old Mill	3	1	2014-06-10, 2014-07-09, 2014-07-10

Station Id	NZ Segment	Station Name	Number Of Events	Type	Event Dates
5538	1042220	Hatea at Whareora Rd	3	2	1988-03-07, 2012-03-19, 2023-02-13
46609	1040689	Mangere at Kara Weir	3	3	1976-08-09, 1977-07-20, 1989-11-26
1323	1011596	Takahue at Crene Road	2	3	2022-08-18, 2025-04-04
1335	1006493	Tarawhataroa at Puriri Place	2	2	2007-07-10, 2022-08-18
1335	1006493	Tarawhataroa at Puriri Place	2	2	2007-07-10, 2022-08-18
1351	1012697	Victoria at Victoria Valley Road	2	3	2022-08-18, 2023-05-09
4914	1041554	Ngunguru at Coal Hill Lane Br	2	1	2020-07-18, 2023-02-13
45903	1062521	Topuni at Old North Rd	2	1	1980-03-15, 1984-08-15
46020	1063284	Hakaru at Topuni Creek Farm	2	1	2023-02-14, 2023-02-24
46660	1038715	Puketurua at Puketitoi	2	1	1967-02-02, 1970-11-03
46902	1035723	Waipoua at SH12	2	3	2007-07-10, 2014-06-10
48015	1013115	Mangamuka at Gorge	2	3	1986-01-25, 1988-03-10
1314	1006270	Awanui at Waikuruki	1	2	19/08/2022
1330	1006331	Awanui at Slackline	1	2	23/01/1980
1909	1007924	Peria at Honeymoon Valley	1	2	13/01/1976
3436	1017107	Waipapa at Doonside Road	1	1	31/08/2014
3503	1016338	Puketotara at Backblocks	1	3	31/07/1979
3518	1016442	Waiwhakangarongaro at Baxters	1	2	20/03/1981
3806	1023578	Kawakawa at SHBr	1	2	4/04/1968
5513	1041582	Glenbervie at Quarry	1	3	20/07/1977
5519	1042267	Waiarohia at Russell Rd	1	2	17/02/1966
5659	1048742	Otaika at Kay	1	3	13/02/2023
6004	1055789	Ahuroa at Rowntrees	1	2	17/07/1973
46645	1046866	Kokopu at McBeths	1	3	8/06/1983
47527	1021073	Opahi at Pond	1	2	17/02/1966